Cdc48 Co-Factor Shp1 Regulates Signal-Induced SCF^{Met30} Disassembly

Linda Lauinger [1], Karin Flick [1], James L. Yen [1,2], Radhika Mathur [1,3] and Peter Kaiser [1,*]

[1] Department of Biological Chemistry, School of Medicine, 240D Medical Science I
University of California, Irvine, CA 92697-1700, USA
[2] Present Address: NeoGenomics laboratories
[3] Present Address: Beckman Coulter

* Correspondence: pkaiser@uci.edu

Abstract

Organisms can adapt to a broad spectrum of sudden and dramatic changes in their environment. These abrupt changes are often perceived as stress and trigger responses that facilitate survival and eventual adaptation. The ubiquitin proteasome system (UPS) is involved in most cellular processes. Unsurprisingly, components of the UPS also play crucial roles during various stress response programs. The budding yeast E3 SCF^{Met30} is an essential Cullin-RING ubiquitin ligase that connects metabolic and heavy metal stress to cell cycle regulation. Cadmium exposure results in the active dissociation of the F-box protein Met30 from the core ligase leading to SCF^{Met30} inactivation. Consequently, SCF^{Met30} substrate ubiquitylation is blocked and triggers a downstream cascade to activate a specific transcriptional rescue program. Signal-induced dissociation is initiated by autoubiquitylation of Met30 and serves as a recruitment signal for the AAA-ATPase Cdc48/p97, which actively disassembles the complex. Here we show that the UBX cofactor Shp1/p47 is an additional key element for SCF^{Met30} disassembly during heavy metal stress. Although the cofactor can directly interact with the ATPase, Cdc48 and Shp1 are recruited independently to SCF^{Met30} during cadmium stress. An intact UBX domain is crucial for effective SCF^{Met30} disassembly, and a concentration threshold of Shp1 recruited to SCF^{Met30} needs to be exceeded to initiate Met30 dissociation. The latter is likely related to Shp1-mediated control of Cdc48 ATPase activity. This study identifies Shp1 as the crucial Cdc48 cofactor for signal-induced, selective disassembly of a multi-subunit protein complex for down-regulation of its activity.

Significance Statement

Ubiquitylation affects many important cellular processes, and has been linked to a number of human diseases including cancer. It has become a synonym for protein degradation, however ubiquitin also has major signaling functions. Understanding the molecular concepts that govern ubiquitin signaling to design diagnostics and therapeutics is of great importance. The cadmium-induced inactivation of the E3 SCF^{Met30} via the disassembly of the multi-subunit ligase complex, illustrates a critical example for non-proteolytic signaling pathways of ubiquitylation. Dissociation is triggered by autoubiquitylation of the F-box protein Met30, which is the recruiting signal for the highly conserved AAA-ATPase Cdc48/p97. Here we present evidence that the UBX cofactor Shp1/p47 is critical for this ubiquitin-dependent, active remodeling of a multi-protein complex in response to a specific environmental signal.

Introduction

The maintenance of protein homeostasis is crucial for eukaryotic cells. The post-translational modification of a protein by ubiquitin conjugation was first described as the major non-lysosomal mechanism by which proteins are targeted for degradation (1). However, destruction of proteins via the proteasomal pathway is only one of many outcomes upon ubiquitylation. The fate of a protein is decided depending on how many ubiquitin molecules are covalently attached to its amino acid residues, and in which fashion ubiquitin chains are formed. The outcomes can be versatile and, for example, influence abundance, activity, or localization of proteins (2–5). Thus, next to degradation, ubiquitylation has major signaling tasks and understanding its influence on cellular function is of central significance. The process of ubiquitin conjugation requires the coordinated reaction of the E1-E2-E3 enzyme cascade. E3 ligases mediate the final step of substrate specific conjugation (6–8). E3s are the most diverse components in the ubiquitylation machinery and are divided in several classes. The largest group is represented by the multi-subunit cullin-RING ligases (CRLs), which include the well-studied subfamily of SCF (Skp1-Cullin-F-box) ligases (9, 10). SCFs are composed of four principal components: The RING finger protein Rbx1, the scaffold Cul1, and the linker Skp1 that forms an association platform with different substrate-specific F-box proteins (11, 12).

The punctual degradation of several SCF substrates is essential to ensure normal cell growth. Hence, alterations in SCF component expression or function can often be linked to cancer and other diseases (13, 14). This highlights the importance to better understand SCF ligase regulation and enable their therapeutic targeting. It has long been thought that ubiquitylation by SCF ligases is regulated at the level of substrate binding (11, 15). However, an additional mode of CRL regulation was recently discovered. Specific SCF ligases can be inhibited by signal-induced dissociation of the F-box subunit from the core ligase (16, 17). The best studied example is SCF^{Met30}, which controls ubiquitylation of a number of different substrates (16, 18–20). However, the transcriptional activator Met4 and the cell-cycle inhibitor Met32 are the most critical ones. Together they orchestrate induction of cell cycle arrest and activation of a specific transcriptional response during nutritional or heavy metal stress. This stress response protects cellular integrity, restores normal levels of sulfur containing metabolites, and activates a defense system for protection against heavy metal stress (21–26). Under normal growth conditions SCF^{Met30} mediates Met4 and Met32 ubiquitylation. Even though both carry a classical canonical destruction signal, only Met32 is degraded via the proteasomal pathway. Met4 in contrast is kept in an inactive state by the attached ubiquitin chain (27, 28). Both, nutrient and heavy metal stress block SCF^{Met30} dependent ubiquitylation of Met4 and Met32, however through profoundly distinctive mechanisms. Nutrient stress prevents the interaction between the SCF^{Met30} ligase and its substrate following the canonical mode of regulation. In contrast, cadmium stress, leads to active dissociation of the F-box subunit Met30 from the core ligase (21, 22). Remarkably, dissociation is initiated by autoubiquitylation of the F-box protein Met30, which serves as the recruiting signal for the highly conserved AAA-ATPase Cdc48/p97 (16). Importantly, ubiquitin-

dependent recruitment of Cdc48 and dissociation of Met30 from the core ligase is independent of proteasomal degradation (16).

Cdc48 is involved in many diverse cellular pathways as extraction of unfolded proteins from the ER (29, 30), discharge of membrane bound transcription factors (31, 32) or chromatin-associated protein extraction (33–38) to only name a few. However, Cdc48 itself rarely displays substrate specificity. An ensemble of regulatory cofactors tightly control functions of the ATPase by recruiting it to different cellular pathways (39–41). Shp1 (**S**uppressor of **H**igh copy protein **P**hosphatase 1 or p47 in mammals) is part of the UBA-UBX family of Cdc48 substrate recruiting adaptors (42). The UBA domain binds ubiquitin, with a preference for multi-ubiquitin chains (43, 44). The central SEP (**S**hp1/**E**yeless/**P**47) domain is involved in trimerization of the cofactor (45, 46), and the UBX domain is structurally similar to ubiquitin and directly interacts with Cdc48 by mimicking a mono-ubiquitylated substrate (47–50). N-terminal of the UBX domain, a short hydrophobic sequence in Shp1 represents an additional Cdc48 binding motif (BS1) (41, 48). More than one binding site allows Shp1 to interact with the ATPase in a bipartite fashion (41, 51).

In yeast, Shp1 is involved in Cdc48-dependent protein degradation via the UPS (47). The $Cdc48^{Shp1}$ complex also interacts with the ubiquitin-fold autophagy protein Atg8 and is a component of autophagosome biogenesis (52). The best studied function of Shp1 lays in the positive regulation of protein phosphatase 1 (Glc7) essential for cell cycle progression (53, 54). Hence, deletion of Shp1 leads to a severe growth phenotype and cells are prone to genomic instability (47, 54, 55). Here we present evidence that next to Cdc48, Shp1 is the crucial cofactor for SCF^{Met30} disassembly in response to heavy metal stress. We identified the very C-terminal 22 amino acids to be important for disassembly. Surprisingly, Cdc48 and Shp1 get recruited independently into SCF^{Met30} during cadmium stress, and recruitment depends on SCF^{Met30} autoubiquitylation. Further, initiation of SCF^{Met30} disassembly is triggered by a Shp1 threshold level necessary for stimulating ATP hydrolysis by Cdc48.

Results

Shp1 is involved in the Cellular Response during Cadmium Stress

The distinct functions of Cdc48/p97 in diverse cellular processes are tightly controlled by a large number of cofactors (40). For mechanical reasons Cdc48 requires at least two anchor points to generate physical force and make Met30 dissociation possible. We selected Shp1 as a candidate cofactor for SCF^{Met30} disassembly, because deletion of Shp1 causes cadmium-sensitivity in yeast cells (16, 47). Immunoprecipitation of Met30 confirmed, that not only the ATPase Cdc48, but also Shp1, is recruited to SCF^{Met30} (Fig 1A). During Cadmium stress Met30 dissociates rapidly from Skp1 as Cdc48 is recruited into SCF^{Met30} ((16) and Fig 1A). By contrast, in a *shp1Δ* (K.O.) strain, Met30 showed severely delayed dissociation kinetics. Additionally, the amount of Cdc48 in complex with Met30 in the absence of Shp1 was significantly increased even under unstressed growth conditions, and accumulated to high levels during cadmium stress (Fig 1A, Suppl. Fig 1 A-D). Increased Cdc48 binding indicates that the dissociation complex intermediate is trapped in *shp1Δ* mutants, and importantly,

that Shp1 is not required for Cdc48 recruitment, but to trigger Cdc48-catalyzed Met30 dissociation (Fig1A, Suppl. Fig 1A-D).

Under normal growth conditions SCF^{Met30} facilitates the ubiquitylation of Met4 and thereby represses the cadmium related stress response (21, 22) Cadmium-triggered dissociation of Met30 blocks Met4 ubiquitylation, leading to cell cycle arrest and induction of the transcription of glutathione and sulfur amino acid biosynthesis regulating genes (25). Accordingly, in the absence of Shp1, Met4 remained ubiquitylated during cadmium stress, confirming that Shp1 is involved in SCF^{Met30} inactivation (Fig 1B). Further, the lack of Met4 activation in the absence of Shp1 is reflected in blunted cadmium-induced Met4 target gene activation (Fig 1C). These results and cadmium hypersensitivity of *shp1Δ* cells (16, 47) suggest, that Shp1 is critical for the Met4-mediated cadmium stress program.

However, Shp1 is essential for normal mitotic progression and *shp1Δ* mutants grow very slowly ((54),Suppl. Fig 1E) or are inviable in certain strains (47). Thus, as with all mutations that severely compromise cell proliferation we were concerned that *shp1Δ* deletion strains acquired compensatory mutations that could lead to misinterpretation of results (56). Therefore, we decided to use the *Auxin Inducible Degron* (AID) system (57, 58) which allowed us to acutely down-regulate Shp1 protein levels. Auxin (IAA) mediates the interaction of the F-box protein Tir1 and an AID-tagged protein leading to the ubiquitylation and proteasomal degradation of the substrate. Accordingly, Shp1 was tagged with a 3xHA-AID-fragment and co-expressed with OsTir in the presence of IAA. Within 30 min of IAA exposure Shp1-AID levels were significantly decreased (Suppl. Figure 1 F). Even though Shp1 levels were severely down-regulated for several hours, no significant growth defect was observed (Suppl. Fig 1G), indicating, that the remaining Shp1 amount was enough to fulfill its function in mitotic progression. Next, we compared cadmium-induced Met30 dissociation between Shp1 knock out and auxin-mediated knock down strains. When Shp1 levels were low (< 10% of endogenous amount) cadmium-induced Met30 dissociation was compromised. However, this dissociation phenotype was not as pronounced as in the complete absence of Shp1 (Fig 1D, Suppl. Fig 1H). Taken together, these results further support a role of Shp1 in SCF^{Met30} regulation during heavy metal stress.

Mutation of Functional Domains in Shp1

Several conserved functional domains have been characterized in Shp1 and its mammalian orthologue p47 (41). To evaluate contribution of these domains in SCF^{Met30} disassembly, we mutated functional motifs in Shp1 (Fig2 A, Suppl. Fig 2A). Shp1 is believed to be constitutively associated with Cdc48 to fulfill its reported cellular functions (48, 51, 52). To disrupt the $Cdc48^{Shp1}$ complex we mutated Cdc48 interaction motifs (CIM1 & 2) in Shp1 (Fig 2A, Suppl. Fig 2A,B). The CIM2 motif is embedded in the ubiquitin like UBX domain, which forms the C-terminus of Shp1. The cofactor contains additional proposed binding sites distal of the CIM2 motif (http://www.ebi.ac.uk/interpro/ and Suppl. Fig 2A). To disrupt the UBX domain without affecting the CIM2 region, we removed only the last 22 residues, which should result in decreased Cdc48 binding (Fig 2A, Suppl. Fig 2A). Note that we refer to this 22 residue deletion as ΔUBX_{Ct}. Cadmium induces auto-ubiquitylation of Met30 and is

a recruitment signal for Cdc48 (16). The UBA domain, which forms the N-terminus of Shp1, is a prototypic ubiquitin binding domain and was thus a candidate to mediate ubiquitin-dependent recruitment of Cdc48 and/or Shp1. All mutations were generated at the endogenous gene locus using CRISPR-based genome editing. Cells carrying Shp1 with ΔCIM1 and ΔCIM2 mutations showed identical behavior in initial experiments (Suppl. Fig 2C-E). Therefore, we continued our studies only with the Shp1ΔCIM2 mutants. All Shp1 variants showed similar expression levels (Fig 2B). In contrast to *shp1Δ* cells, at 30°C none of the strains showed substantial growth defects (Fig 2C). We noticed significantly reduced Met30 levels in *shp1Δ* mutants, which was not observed in any of the domain mutations (Fig. 2C). Met30 protein stability was not affected, but *shp1Δ* mutants showed reduced *MET30* RNA expression (Suppl. Fig 2F,G). The reason for the expression effect is unknown. We next analyzed Cdc48 interaction with the various Shp1 mutants. As expected, deletion of the UBA domain did not affect Cdc48 interaction. However, consistent with previous reports (54) deletion of CIM2 and UBX_{Ct} domains in Shp1 showed dramatically decreased, but not completely abolished, Cdc48 binding (Fig 2D).

The UBX domain of Shp1 is required for SCF^{Met30} Disassembly during Cadmium Stress

We next tested the Shp1 variants for cadmium sensitivity. As previously shown, the *shp1Δ* deletion mutants were hypersensitive towards cadmium exposure (16, 47) All Shp1 variants tolerated cadmium exposure, except ΔUBX_{Ct} cells, which exhibited a less prominent but evident sensitivity (Fig 3A). Cadmium sensitivity caused by defects in the SCF^{Met30} system is due to a lack of Met4 activation and the resulting lack of induction of a defense program mediated by Met4-dependent gene transcription. Consistent with the cadmium sensitivity of *shp1-Δubx*$_{Ct}$ mutants they could not activate Met4 demonstrated by maintained ubiquitylated Met4 during heavy metal stress. All other Shp1 variants, like wild-type cells, responded by activating Met4 upon cadmium exposure (Fig 3B). These findings were further confirmed by analysis of cadmium-induced Met4 target genes. Shp1ΔUBA and ΔCIM2 showed induction of *MET25* and *GSH1* similar to the wild-type Met4. In contrast, *shp1-Δubx*$_{Ct}$ mutants did not efficiently activate gene expression, consistent with persistent Met4 ubiquitylation and cadmium sensitivity of this mutant (Fig 3C).

In addition to heavy metal stress methionine starvation blocks Met4 ubiquitylation and induces a similar transcriptional response program (25). Thus, we next asked, if Shp1 was required solely during heavy metal stress for Met4 activation. The expression of Met4-dependent genes in response to methionine starvation was not affected in any *shp1* mutatnts (Suppl. Fig 3A). This demonstrates a cadmium exclusive role of Shp1 for the activation of Met4, and is consitstent with the different mode of Met4 activation during cadmium and methionine stress. While cadmium stress inactivates SCF^{Met30} by active dissociation of Met30 from the core ligase, methionine stress retains an intact SCF^{Met30} complex, but blocks association of the ubiquitin ligase with its substrate Met4 (16, 21, 22) We next evaluated cadmium-induced SCF^{Met30} disassembly in *shp1* mutants. *shp1-Δubx*$_{Ct}$ mutants showed very

slow Met30 dissociation, and the majority of Met30 remained in complex with the core ligase during heavy metal stress (Fig 3D). In contrast, all other mutants were indistinguishable from wild-type cells (Fig. 3D). In summary our results indicate, that an intact UBX domain of Shp1 is required for SCF^{Met30} disassembly during cadmium stress. Importantly, even though both ΔCIM2 and ΔUBX_{Ct} mutantions showed decreased Shp1 interaction with Cdc48 to a similar extent (Fig 2D), only *shp1-Δubx*$_{Ct}$ mutants exhibit a dissociation phenotype. Hence, the role of Shp1 in SCF^{Met30} during heavy metal stress is independent of a stable Cdc48-Shp1 interaction.

Met30 Dissociation kinetics during Heavy Metal Stress are dependent on Shp1 Abundance

We next had monitored Cdc48 and co-factor recruitment, as well as kinetics of SCF^{Met30} disassembly in the *shp1-Δubx*$_{Ct}$ mutants. Immunoprecipitated SCF^{Met30} still formed a complex with Cdc48 and Shp1ΔUBX_{Ct} under unstressed growth conditions (Fig 4A), further supporting that stable Cdc48-Shp1 binding is not required for recruitment of either. Consistent with previous experiments, during heavy metal stress disassembly kinetics of SCF^{Met30} in *shp1Δ* and *shp1-Δubx*$_{Ct}$ mutants were severely delayed (Fig 4A, Suppl. Fig 4A). Surprisingly, similar to *shp1Δ*, under normal growth conditions the amount of Cdc48 in complex with Met30 was significantly increased in *shp1-Δubx*$_{Ct}$ mutants (Fig 4A; Suppl. Fig 4D). The increased steady state binding of Cdc48 to SCF^{Met30} in *shp1* mutants may be a result of the blocked dissociation and likely reflects accumulation of a dissociation intermediate (Fig 4A, Suppl. Fig 4C). Shp1ΔUBX_{Ct} does not efficiently interact with Cdc48 (Fig. 2D), yet both Cdc48 and Shp1ΔUBX_{Ct} are recruited to SCF^{Met30}, even though mutation of the UBX domain reduced overall recruitment efficiency (Fig. 4A). Shp1ΔUBX_{Ct} recruitment to SCF^{Met30} was only about 2-fold increased after 40 minutes cadmium exposure, whereas wild-type Shp1 was 6-fold enriched (Fig 4A, Suppl. Fig 4B). Importantly, decreased enrichment was not due to partial loss of Cdc48 binding, because Shp1ΔCIM2, which shows a similar reduction in Cdc48 binding (Fig. 2D), was recruited to SCF^{Met30} at similar levels as wild-type Shp1 (Suppl. Fig 4E). These results suggest that both Cdc48 and Skp1 are independently recruited to SCF^{Met30}, but their interaction through the UBX domain on Sph1 is necessary to stabilize the complex and mediate Met30 dissociation. The altered dissociation kinetics in *shp1-Δubx*$_{Ct}$ mutants are reflected in delayed Met4 activation indicated by persistent Met4 ubiquitylation (Fig. 4B). Notably, Met4 activation was even more delayed when *SPH1* was completely deleted (Fig 4B). This observation explains the slightly stronger transcriptional response of *shp1-Δubx*$_{Ct}$ mutants compared to *shp1Δ* cells (Fig 3C, Suppl. Fig 3A).

The concentration of Shp1ΔUBX_{Ct} in the SCF^{Me30}/Cdc48 complex after heavy metal exposure was considerably lower than that of wild-type Shp1 (Fig 4A, Suppl. Fig 4B), suggesting that a threshold concentration may control initiation of the dissociation process. We therefore investigated if Shp1 abundance bound to the SCF^{Met30} complex during cadmium stress correlated with Met30 dissociation. The AID system enabled us to titrate various Shp1 levels, ranging from endogenous amounts to about ten-fold lower (Fig 4C). Met30 dissociation was attenuated when Shp1-AID levels were decreased, such that the lower Shp1-AID levels were, the more Met30 remained in complex with the core ligase.

Quantification revealed, a correlation between Shp1 abundance and cadmium-induced SCF^{Met30} disassembly (Fig 4D, Suppl. Fig 4F). A significant dissociation defect was only observed, when Shp1-AID levels were less than 20%, suggesting that SCF^{Met30} regulation during cadmium stress is dependent on Shp1 abundance in the complex. However, Shp1 amounts recruited to the SCF^{Me30}/Cdc48 complex necessary for complete SCF^{Me30} disassembly (Fig. 4C, 1h IAA) were significantly lower than recruited Shp1ΔUBX$_{Ct}$ levels (Fig 4A, Suppl. Fig 4H). Thus, the defect of Met30 dissociation observed in *shp1-Δubx$_{Ct}$* mutants is not due to reduced Shp1ΔUBX$_{Ct}$ recruitment, but reflect requirement of UBX mediated interaction with Cdc48 to stabilize the complex and trigger dissociation.

Discussion

Cdc48 is an exceptionally versatile protein in eukaryotic cells and substrate specificity is thought to depend on co-factors (40). During heavy metal stress Cdc48 plays a critical role in signal-induced disassembly of the SCF^{Met30} ubiquitin ligase complex (16). Our results show that the UBA-UBX co-factor Shp1 is critical for this process. Like Cdc48, Shp1 is recruited into SCF^{Met30} upon cadmium exposure (Fig1A, Suppl. Fig 1B). Interestingly, the prominent heterodimeric Ufd1/Npl4 cofactor pair also gets recruited into SCF^{Met30} under heavy metal stress conditions (Suppl. Fig 5 A,B). However, temperature-sensitive *ufd1-2* and *npl4-1* mutants do not exhibit cadmium sensitivity, nor Met4 activation defects, or a dissociation phenotype during heavy metal stress (16). Likely cadmium-induced recruitment of Ufd1/Npl4 reflects their canonical function in this system and is necessary for targeting dissociated Met30 for degradation to the proteasome. Cadmium stress generates an excess of ubiquitylated "Skp1-free" Met30, which is rapidly degraded via a Cdc53-dependent, but Skp1-independent proteolytic pathway (59). Consistent with this model, Met30 that cannot associate with Skp1 ($Met30^{\Delta F\text{-}box}$), which serves as a surrogate to mimic dissociated Met30, is stabilized in temperature-sensitive *ufd1-2* and *npl4-2* mutants (Suppl. Fig. 5 C). Therefore, we speculate that there might be two populations of Cdc48 complexes involved in processing the SCF^{Met30} during cadmium stress. The $Cdc48^{Shp1}$ complex is required for the disassembly of the SCF^{Met30}, and $Cdc48^{Ufd1/Npl4}$ for degradation of unbound Met30 via the proteasomal pathway.

Met30 protein levels in the *shp1*Δ were significantly decreased compared to wild-type cells (Fig 1A, Fig 2B). Shp1 is involved in the degradation of a Cdc48-dependet model substrate (47), but the half-life of Met30 is unaffected in *shp1Δ* cells and all other *shp1* variants we tested (Suppl. Fig 2F). However, *MET30* RNA levels were significantly decreased in the knock out strain (Suppl. Fig 2G). Accordingly, low Met30 protein levels are due to a transcriptional defect. Since all other Shp1 variants showed normal RNA levels, we hypothesize that altered transcription might be associated with other aspects of Shp1 function (54).

Closer examination of functional domains in Shp1 revealed several interesting findings. Met30 is autoubiquitylated during heavy metal stress (16), therefore we considered that the UBA with its ubiquitin binding ability might play a role in Shp1 recruitment Additionally, it is proposed that UBA domains can inhibit ubiquitin chain elongation (60). Our hypothesis, that the UBA domain might bind

to autoubiquitylated Met30 and keep the K48-liked chain short was not confirmed. Surprisingly, deletion of the UBA in Shp1 did not show any cadmium specific phenotype and is not required for SCF^{Met30} or Met4 regulation (Fig 3).

Shp1 is believed to be constitutively bound to Cdc48 to fulfill its cellular tasks (48, 51, 52). Therefore, we were surprised to find that Cdc48 and Shp1 were independently recruited to SCF^{Met30} upon cadmium exposure (Fig 1A & Fig 3A, Suppl. Fig 4E). Furthermore, the interaction of Shp1ΔCIM2 with Cdc48 is dramatically compromised, but not completely abolished (Fig 2D). Yet, *shp1-Δcim2* mutants are capable to dissociate and effectively inactivate SCF^{Met30} (Fig 3). In addition, the recruitment of Shp1ΔCIM2 to the E3 ligase during heavy metal stress is unaffected (Suppl. Fig 4E). Conversely, in the absence of Shp1, Cdc48 is still recruited to SCF^{Met30} during cadmium stress (Fig 1A). These findings suggest two independent binding sites for Cdc48 and Shp1 on SCF^{Met30}, and supports the idea considering mechanical transmission of forces for separation of Met30 requiring at least two anchor points.

In contrast to *shp1-Δcim2* mutants, truncation of the last 22 residues (ΔUBX_{Ct}), which led to similar defects in Cdc48 binding, resulted in severely impaired Met30 dissociation and blunted the entire cadmium stress response. The recruitment of $Shp1\Delta UBX_{Ct}$ into SCF^{Met30} was reduced (Fig 4A), but not to an extent that would block SCF^{Met30} disassembly, based on titration experiments with wild-type Shp1 (Fig. 4C and D, Suppl. Fig 4H). Weakened interaction with Cdc48 was not the reason for altered recruitment or failure to dissociate Met30, because Shp1ΔCIM2 is equally deficient in Cdc48 interaction, yet recruitment to SCF^{Met30} and Met30 dissociation is undistinguishable from wild-type cells (Suppl. Fig 4E). Our results more likely suggest that the UBX domain is important for proper assembly of a functional disassembly complex to stimulate the Cdc48 ATPase activity and generate the required force for Met30 dissociation. In addition, the residues we deleted are sites for potential posttranslational modifications in the human orthologue p47 (61, 62). Lack of these sites might distort the disassembly complex. Future mass spectrometry analyses will help to identify potential additional cofactors and posttranslational modifications required for cadmium response.

Under normal growth conditions, the amount of Cdc48 in complex with Met30 in the absence of Shp1 was significantly increased (Fig 1A, Suppl. Fig 1D). This was also the case for the $Shp1\Delta UBX_{Ct}$ variant (Fig 3A, Suppl. Fig 3D). The higher steady state binding under normal growth resulted in reduced fold enrichment of Cdc48 during cadmium stress when compared to wild-type cells, even though total bound levels were higher in *shp1* mutants (Fig 1A, Fig 3A). Because Shp1 is required for SCF^{Met30} but not Cdc48 recruitment, the observed complex in *shp1* mutants is likely a dissociation intermediate, blocked just before the step of SCF^{Met30} disassembly. The increased association of Cdc48 with SCF^{Met30} in *shp1* mutants under normal growth conditions indicates that low level Met30 dissociation is ongoing without exogenous stress. This process may be part of a quality control mechanism that monitors proper assembly of the ubiquitin ligase complex.

Cdc48/p97 can bind to ubiquitin directly *in vitro* (31). However, UBX cofactors are thought to be adaptors that regulate the interaction between Cdc48 and its substrates proteins (48). Under normal

growth conditions Met30 is ubiquitylated at low levels, but cadmium stress drastically increases Met30 autoubiquitylation (16). This autoubiquitylation is the recruitment signal for Cdc48 and given that Cdc48 recruitment is independent of Shp1 and Npl4/Ufd1 (Fig 1A, Fig3A) (16), the ATPase likely interacts with ubiquitylated Met30 directly. However, Shp1 is required to properly orient the complex, activate the ATPase activity, and provide a second attachment point for transmission of the mechanical force.

Initially, we used the AID system to temporally down-regulate Shp1 levels to study acute loss of Shp1 function and eliminate possible indirect effects caused by secondary mutations acquired by the *shp1Δ* deletion strain. However, it also became a handy tool to closer examine concentration dependency of Shp1 in SCF^{Met30} during cadmium stress. Upon auxin addition, Shp1-AID exhibited a half-life of less than 30 min (Suppl. Fig 1F, Fig 4C,D). With decreased Shp1-AID levels, SCF^{Met30} dissociation kinetics were significantly slower (Fig 1D). Moreover, by titrating Shp1-AID levels, a correlation between Shp1 abundance and disassembly kinetics became obvious (Fig 4C,D). Although, Shp1 abundance decreased with the duration of auxin incubation, the recruitment rate of Shp1 to SCF^{Met30} increased (Fig 4C; Suppl. Fig 4 F,G). This phenomenon is likely related to a need for a minimum concentration of Shp1 in the dissociation complex to activate Cdc48. When first discovered, human p47 was initially described as an inhibitor of p97 activity (63). However, a more recent study showed a more complex mechanism of ATPase regulation by the cofactor. *In vitro*, p47 showed a biphasic inhibition of p97 (64). ATPase activity was strongly inhibited at relatively low p47 concentration (phase 1). However, at higher stoichiometric amounts of the cofactor, inhibition was relived (phase 2). The authors suggest, that in phase1 p47 is found as a monomer on p97. Whereas, phase 2 reaches maximum activity, when trimeric p47 is formed (64). We hypothesize, that at low amounts Shp1 facilitates maximum inhibition of Cdc48 ATPase activity. Upon cadmium exposure, Shp1 is recruited to SCF^{Met30}, increasing the local concentration of the cofactor. This increase might lead to Shp1 trimerization and stimulation of ATP hydrolysis followed by separation of Met30 from the core ligase. Future experiments will need to address this hypothesis.

Our study shows a critical role for the UBA-UBX Cofactor Shp1 during heavy metal stress. The ATPase Cdc48 and Shp1 are recruited independently to SCF^{Met30} during cadmium stress, but interaction through the UBX domain of Shp1 is necessary to activate the dissociation complex and catalyze dissociation of Met30. These results provide insight into ubiquitin-dependent, signal-induced, active remodeling of multi-protein complexes to modulate activity.

Acknowledgments

We thank S. Jentsch, T. Rapoport, P. Silver, and R. Hampton for yeast strains; R. Deshaies, W. Harper, M. Tyers, T. Sommer, and E. Jarosch for antibodies.

This work was supported by the National Institute of Health grant R01 GM-066164 to P.K. and the Hitachi-Nomura Award to L. L..

References

1. H. Nakatogawa, K. Suzuki, Y. Kamada, Y. Ohsumi, Dynamics and diversity in autophagy mechanisms: Lessons from yeast. *Nat. Rev. Mol. Cell Biol.* **10**, 458–467 (2009).
2. A. Hershko, A. Ciechanover, THE UBIQUITIN SYSTEM. *Annu. Rev. Biochem.* (1998) https:/doi.org/10.1146/annurev.biochem.67.1.425.
3. A. Varshavsky, Regulated protein degradation in *Trends in Biochemical Sciences*, (2005) https:/doi.org/10.1016/j.tibs.2005.04.005.
4. D. Finley, H. D. Ulrich, T. Sommer, P. Kaiser, The ubiquitin-proteasome system of Saccharomyces cerevisiae. *Genetics* **192**, 319–360 (2012).
5. D. Komander, M. Rape, The Ubiquitin Code. *Annu. Rev. Biochem.* **81**, 203–229 (2012).
6. O. Kerscher, R. Felberbaum, M. Hochstrasser, Modification of Proteins by Ubiquitin and Ubiquitin-Like Proteins. *Annu. Rev. Cell Dev. Biol.* (2006) https:/doi.org/10.1146/annurev.cellbio.22.010605.093503.
7. C. M. Pickart, M. J. Eddins, Ubiquitin: Structures, functions, mechanisms. *Biochim. Biophys. Acta - Mol. Cell Res.* (2004) https:/doi.org/10.1016/j.bbamcr.2004.09.019.
8. A. Varshavsky, The Ubiquitin System, an Immense Realm. *Annu. Rev. Biochem.* **81**, 167–176 (2012).
9. R. J. Deshaies, C. A. P. Joazeiro, RING Domain E3 Ubiquitin Ligases. *Annu. Rev. Biochem.* **78**, 399–434 (2009).
10. D. M. Duda, *et al.*, Structural regulation of cullin-RING ubiquitin ligase complexes. *Curr. Opin. Struct. Biol.* (2011) https:/doi.org/10.1016/j.sbi.2011.01.003.
11. M. D. Petroski, R. J. Deshaies, Function and regulation of cullin-RING ubiquitin ligases. *Nat. Rev. Mol. Cell Biol.* (2005) https:/doi.org/10.1038/nrm1547.
12. J. Jin, *et al.*, Systematic analysis and nomenclature of mammalian F-box proteins. *Genes Dev.* (2004) https:/doi.org/10.1101/gad.1255304.
13. A. Ciechanover, A. L. Schwartz, Ubiquitin-mediated degradation of cellular proteins in health and disease. *Hepatology* **35**, 3–6 (2002).
14. M. Schmidt, D. Finley, Regulation of proteasome activity in health and disease. *Biochim. Biophys. Acta - Mol. Cell Res.* **1843**, 13–25 (2014).
15. D. Skowyra, K. L. Craig, M. Tyers, S. J. Elledge, J. W. Harper, F-box proteins are receptors that recruit phosphorylated substrates to the SCF ubiquitin-ligase complex. *Cell* **91**, 209–219 (1997).
16. J. L. Yen, *et al.*, Signal-induced disassembly of the scf ubiquitin ligase complex by cdc48/p97. *Mol. Cell* **48**, 288–297 (2012).
17. F. N. Li, M. Johnston, Grr1 of Saccharomyces cerevisiae is connected to the ubiquitin proteolysis machinery through Skp1: Coupling glucose sensing to gene expression and the cell cycle. *EMBO J.* **16**, 5629–5638 (1997).
18. P. Kaiser, N.-Y. Su, J. L. Yen, I. Ouni, K. Flick, The yeast ubiquitin ligase SCF^{Met30}: Connecting

environmental and intracellular conditions to cell division. *Cell Div.* **1** (2006).

19. I. Ouni, K. Flick, P. Kaiser, A transcriptional activator is part of an SCF ubiquitin ligase to control degradation of its cofactors. *Mol Cell* **40**, 954–964 (2010).
20. A. Rouillon, R. Barbey, E. E. Patton, M. Tyers, D. Thomas, Feedback-regulated degradation of the transcriptional activator Met4 is triggered by the SCF(Met30)complex. *Embo J* **19**, 282–294 (2000).
21. J. L. Yen, N. Y. Su, P. Kaiser, The yeast ubiquitin ligase SCFMet30 regulates heavy metal response. *Mol. Biol. Cell* (2005) https:/doi.org/10.1091/mbc.E04-12-1130.
22. R. Barbey, *et al.*, Inducible dissociation of SCFMet30 ubiquitin ligase mediates a rapid transcriptional response to cadmium. *EMBO J.* (2005) https:/doi.org/10.1038/sj.emboj.7600556.
23. E. E. Patton, *et al.*, SCF Met30 -mediated control of the transcriptional activator Met4 is required for the G 1 – S transition. **19**, 1613–1624 (2000).
24. G. L. Wheeler, E. W. Trotter, I. W. Dawes, C. M. Grant, Coupling of the Transcriptional Regulation of Glutathione Biosynthesis to the Availability of Glutathione and Methionine via the Met4 and Yap1 Transcription Factors. *J. Biol. Chem.* (2003) https:/doi.org/10.1074/jbc.M310156200.
25. P. Kaiser, N. Y. Su, J. L. Yen, I. Ouni, K. Flick, The yeast ubiquitin ligase SCFMet30: Connecting environmental and intracellular conditions to cell division. *Cell Div.* **1**, 1–8 (2006).
26. E. Carrillo, *et al.*, Characterizing the roles of Met31 and Met32 in coordinating Met4-activated transcription in the absence of Met30. *Mol. Biol. Cell* (2012) https:/doi.org/10.1091/mbc.E11-06-0532.
27. K. Flick, S. Raasi, H. Zhang, J. L. Yen, P. Kaiser, A ubiquitin-interacting motif protects polyubiquitinated Met4 from degradation by the 26S proteasome. *Nat. Cell Biol.* (2006) https:/doi.org/10.1038/ncb1402.
28. I. Ouni, K. Flick, P. Kaiser, A Transcriptional Activator Is Part of an SCF Ubiquitin Ligase to Control Degradation of Its Cofactors. *Mol. Cell* (2010) https:/doi.org/10.1016/j.molcel.2010.11.018.
29. R. Y. Hampton, ER-associated degradation in protein quality control and cellular regulation. *Curr. Opin. Cell Biol.* (2002) https:/doi.org/10.1016/S0955-0674(02)00358-7.
30. N. O. Bodnar, T. A. Rapoport, Molecular Mechanism of Substrate Processing by the Cdc48 ATPase Complex. *Cell* **169**, 722-735.e9 (2017).
31. M. Rape, *et al.*, Mobilization of processed, membrane-tethered SPT23 transcription factor by CDC48UFD1/NPL4, a ubiquitin-selective chaperone. *Cell* (2001) https:/doi.org/10.1016/S0092-8674(01)00595-5.
32. N. Shcherbik, D. S. Haines, Cdc48pNpl4p/Ufd1p Binds and Segregates Membrane-Anchored/Tethered Complexes via a Polyubiquitin Signal Present on the Anchors. *Mol. Cell* **25**, 385–397 (2007).

33. K. Acs, *et al.*, The AAA-ATPase VCP/p97 promotes 53BP1 recruitment by removing L3MBTL1 from DNA double-strand breaks. *Nat. Struct. Mol. Biol.* (2011) https:/doi.org/10.1038/nsmb.2188.
34. A. Franz, *et al.*, CDC-48/p97 Coordinates CDT-1 Degradation with GINS Chromatin Dissociation to Ensure Faithful DNA Replication. *Mol. Cell* (2011) https:/doi.org/10.1016/j.molcel.2011.08.028.
35. M. Raman, C. G. Havens, J. C. Walter, J. W. Harper, A Genome-wide Screen Identifies p97 as an Essential Regulator of DNA Damage-Dependent CDT1 Destruction. *Mol. Cell* (2011) https:/doi.org/10.1016/j.molcel.2011.06.036.
36. R. Verma, R. Oania, R. Fang, G. T. Smith, R. J. Deshaies, Cdc48/p97 mediates UV-dependent turnover of RNA Pol II. *Mol. Cell* (2011) https:/doi.org/10.1016/j.molcel.2010.12.017.
37. A. J. Wilcox, J. D. Laney, A ubiquitin-selective AAA-ATPase mediates transcriptional switching by remodelling a repressor-promoter DNA complex. *Nat. Cell Biol.* (2009) https:/doi.org/10.1038/ncb1997.
38. A. Ndoja, R. E. Cohen, T. Yao, Ubiquitin signals proteolysis-independent stripping of transcription factors. *Mol. Cell* **53**, 893–903 (2014).
39. H. Meyer, M. Bug, S. Bremer, Emerging functions of the VCP/p97 AAA-ATPase in the ubiquitin system. *Nat. Cell Biol.* **14**, 117–123 (2012).
40. S. Rumpf, S. Jentsch, Functional division of substrate processing cofactors of the ubiquitin-selective Cdc48 chaperone. *Mol. Cell* **21**, 261–269 (2006).
41. A. Buchberger, H. Schindelin, P. Hänzelmann, Control of p97 function by cofactor binding. *FEBS Lett.* **589**, 2578–2589 (2015).
42. A. Buchberger, From UBA to UBX: New words in the ubiquitin vocabulary. *Trends Cell Biol.* **12**, 216–221 (2002).
43. B. L. Bertolaet, *et al.*, UBA domains of DNA damage-inducible proteins interact with ubiquitin. *Nat. Struct. Biol.* (2001) https:/doi.org/10.1038/87575.
44. C. R. M. Wilkinson, *et al.*, Proteins containing the UBA domain are able to bind to multi-ubiquitin chains. *Nat. Cell Biol.* (2001) https:/doi.org/10.1038/ncb1001-939.
45. F. Beuron, *et al.*, Conformational changes in the AAA ATPase p97-p47 adaptor complex. *EMBO J.* **25**, 1967–1976 (2006).
46. I. Dreveny, *et al.*, Structural basis of the interaction between the AAA ATPase p97/VCP and its adaptor protein p47. *EMBO J.* **23**, 1030–1039 (2004).
47. C. Schuberth, H. Richly, S. Rumpf, A. Buchberger, Shp1 and Ubx2 are adaptors of Cdc48 involved in ubiquitin-dependent protein degradation. *EMBO Rep.* **5**, 818–824 (2004).
48. C. Schuberth, A. Buchberger, UBX domain proteins: Major regulators of the AAA ATPase Cdc48/p97. *Cell. Mol. Life Sci.* **65**, 2360–2371 (2008).
49. P. Kloppsteck, C. A. Ewens, A. Förster, X. Zhang, P. S. Freemont, Regulation of p97 in the ubiquitin-proteasome system by the UBX protein-family. *Biochim. Biophys. Acta - Mol. Cell*

Res. (2012) https:/doi.org/10.1016/j.bbamcr.2011.09.006.

50. G. Alexandru, *et al.*, UBXD7 binds multiple ubiquitin ligases and implicates p97 in HIF1α turnover. *Cell* **134**, 804–816 (2008).
51. R. M. Bruderer, C. Brasseur, H. H. Meyer, The AAA ATPase p97/VCP interacts with its alternative co-factors, Ufd1-Np14 and p47, through a common bipartite binding mechanism. *J. Biol. Chem.* (2004) https:/doi.org/10.1074/jbc.M408695200.
52. R. Krick, *et al.*, Cdc48/p97 and Shp1/p47 regulate autophagosome biogenesis in concert with ubiquitin-like Atg8. *J. Cell Biol.* **190**, 965–973 (2010).
53. S. Zhang, S. Guha, F. C. Volkert, The Saccharomyces SHP1 gene, which encodes a regulator of phosphoprotein phosphatase 1 with differential effects on glycogen metabolism, meiotic differentiation, and mitotic cell cycle progression. *Mol. Cell. Biol.* (1995) https:/doi.org/10.1128/mcb.15.4.2037.
54. S. Böhm, A. Buchberger, The Budding Yeast Cdc48Shp1 Complex Promotes Cell Cycle Progression by Positive Regulation of Protein Phosphatase 1 (Glc7). *PLoS One* **8**, 22–24 (2013).
55. Y. L. Cheng, R. H. Chen, The AAA-ATPase Cdc48 and cofactor Shp1 promote chromosome bi-orientation by balancing Aurora B activity. *J. Cell Sci.* (2010) https:/doi.org/10.1242/jcs.066043.
56. G. Giaever, C. Nislow, The yeast deletion collection: a decade of functional genomics. *Genetics* **197**, 451–65 (2014).
57. K. Nishimura, T. Fukagawa, H. Takisawa, T. Kakimoto, M. Kanemaki, An auxin-based degron system for the rapid depletion of proteins in nonplant cells. *Nat. Methods* **6**, 917–922 (2009).
58. M. Morawska, H. D. Ulrich, An expanded tool kit for the auxin-inducible degr on system in budding yeast. **4**, 1–4.
59. R. Mathur, J. L. Yen, P. Kaiser, Skp1 Independent Function of Cdc53/Cul1 in F-box Protein Homeostasis. *PLoS Genet.* **11**, 1–21 (2015).
60. L. Chen, U. Shinde, T. G. Ortolan, K. Madura, Ubiquitin-associated (UBA) domains in Rad23 bind ubiquitin and promote inhibition of multi-ubiquitin chain assembly. *EMBO Rep.* (2001) https:/doi.org/10.1093/embo-reports/kve203.
61. W. Kim, *et al.*, Systematic and quantitative assessment of the ubiquitin-modified proteome. *Mol. Cell* (2011) https:/doi.org/10.1016/j.molcel.2011.08.025.
62. V. Akimov, *et al.*, Ubisite approach for comprehensive mapping of lysine and n-terminal ubiquitination sites. *Nat. Struct. Mol. Biol.* **25** (2018).
63. H. H. Meyer, H. Kondo, G. Warren, The p47 co-factor regulates the ATPase activity of the membrane fusion protein, p97. *FEBS Lett.* **437**, 255–257 (1998).
64. X. Zhang, *et al.*, Altered cofactor regulation with disease-associated p97/VCP mutations. *Proc. Natl. Acad. Sci.* **112**, E1705–E1714 (2015).

Figure Legends

Figure 1 - Shp1 is involved in the Cellular Response during Cadmium Stress

A) Shp1 is recruited to SCF^{Met30} during Cadmium Stress. In the *shp1Δ* cells (K.O.) dissociation kinetics of Met30 from the core ligase are decreased. Strains expressing endogenous ^{12xMyc}Met30, $Cdc48^{RGS6H}$, Skp1 and $Shp1^{3xHA}$ in the WT or, *shp1* was knocked out (K.O.). WT and K.O. cells were cultured at 30°C in YEPD medium and treated with 100 µM Cadmium and samples were harvested at indicated time points. ^{12xMyc}Met30 was immunoprecipitated and co-precipitated proteins were analyzed by Western blot. B) Shp1 is necessary for Met4 activation during Heavy Metal Stress. Whole cells lysates (Totals) of samples shown in Figure 1A were analyzed by Western blot using a Met4 antibody to follow the ubiquitylation and phosphorylation status of Met4. Tubulin was used as a loading control. C) Cadmium induced gene expression is altered in the absence of Shp1. RNA was extracted from samples shown in Figure 1A. Expression of Met4 target genes *MET25* and *GSH1* was analyzed by RT-PCR and normalized to 18S rRNA levels (n=3), data are represented as mean ±SD. D) Temporal down-regulation of Shp1 shows its importance during Cadmium Stress. Strains expressing endogenous ^{12xMyc}Met30, $Shp1^{3xHA\text{-}AID}$ and the F-Box protein ^{2xFLAG}OsTir under the constitutive ADH promoter were cultured at 30°C in YEPD medium in the absence and presence of 500 µM auxin for 4 hours to down-regulate endogenous Shp1 levels. The Shp1 K.O. strain was not exposed to auxin. Cells were treated with 100 µM Cadmium and samples were harvested after 20 min of heavy metal exposure. ^{12xMyc}Met30 was immunoprecipitated and co-precipitated proteins were analyzed by Western blot. Results shown in A, B and D are representative blots from three independent experiments.

Figure 2 – Characterization of Functional Domains in Shp1

A) Schematic of Shp1 and its known functional domains and motifs. UBA = ubiquitin-associated domain (6-46), SEP = Shp1, eyeless and p47 domain (238-313), UBX = ubiquitin regulatory X domain (346-420), CIM 1&2 = Cdc48-interacting motifs 1 (LGGFSGQGQRL; 304-314 distal of SEP domain also known as BS1) & 2 (FPI; 396-398 in UBX domain). B) Expression levels of Shp1 mutants. Strains expressing endogenous ^{12xMyc}Met30, $Cdc48^{RGS6H}$, Skp1 and WT $Shp1^{3xHA}$ compared to $Shp1^{3xHA}$ mutant variants. ΔUBA = deletion of aa 1-50, ΔCIM2 = aa 396-398 FPI were replaced with GAG, ΔUBX_{Ct} = deletion of aa 401-423 or *shp1* was knocked out (K.O.). Proteins were analyzed by Western blot, tubulin was used as a loading control. C) Shp1 mutants do not show a substantial growth defect at 30°C. Shp1 WT, mutant variants and K.O. strains were grown at 30°C in YEPD medium and samples were taken at indicated time points. Optic Density was measured at 600nm. D) Cdc48 binding is significantly decreased in ΔCIM2 and ΔUBX_{Ct} Shp1 mutants. $SHP1^{3xHA}$ variants were immunoprecipitated and co-precipitation of $Cdc48^{RGS6H}$ was analyzed by Western blot. The Shp1 K.O. strain was used as a background control. Results shown in B and D are representative blots from three independent experiments.

Figure 3 – UBX domain of Shp1 is required for SCF^{Met30} Disassembly during Cadmium Stress

A) Shp1ΔUBX$_{Ct}$ shows sensitivity towards cadmium exposure. For the cell spotting assay indicated strains were cultured to logarithmic growth phase and cells were counted. Serial dilutions were made and spotted onto YEPD plates supplemented with or without 50 µM of cadmium. Plates were incubated for two days at 30°C. B) The UBX domain is important for Met4 activation during heavy metal stress. Strains shown in Figure 3A were cultured at 30°C in YEPD medium treated with 100 µM Cadmium and samples were harvested after 20 min of heavy metal exposure. Whole cell lysates were analyzed by Western blot using a Met4 antibody to follow the ubiquitylation and phosphorylation status of Met4. Tubulin was used as a loading control. C) Insufficient Met4 activation in Shp1 ΔUBX$_{Ct}$ is reflected in *MET25* and *GSH1* RNA levels. Depicted strains were grown at 30°C in YEPD medium treated with 100 µM Cadmium and samples were harvested after 40 min exposure. RNA was extracted and expression of Met4 target genes *MET25* and *GSH1* was analyzed by RT-PCR and normalized to 18S rRNA levels (n=3). data are represented as mean ±SD. D) Shp1 ΔUBX$_{Ct}$ shows altered dissociation kinetics during cadmium stress. ^{12xMyc}Met30 of lysates shown in Figure 3B was subjected to immunoprecipitation and co-precipitated proteins were analyzed by Western blot. Results shown in B and D are representative blots from three independent experiments.

Figure 4 – Met30 Dissociation kinetics during Heavy Metal Stress are dependent on Shp1 Abundance

A) Cadmium-induced recruitment of Shp1 into SCF^{Met30} is significantly decreased in ΔUBX$_{Ct}$ mutant. Strains expressing endogenous ^{12xMyc}Met30, Cdc48^{RGS6H}, Skp1 and WT Shp1^{3xHA} or ΔUBX$_{Ct}$ Shp1^{3xHA} respectively were cultured at 30°C in YEPD medium treated with 100 µM Cadmium and samples were harvested at indicated time points. Whole cells lysates (Totals) were prepared and ^{12xMyc}Met30 was immunoprecipitated and co-precipitated proteins were analyzed by Western blot. B) Shp1ΔUBX$_{Ct}$ shows delayed Met4 activation. Totals shown in Fig 4A were analyzed by Western blot using a Met4 antibody to follow the ubiquitylation and phosphorylation status of Met4. Tubulin was used as a loading control. C) Met30 dissociation kinetics dependent on Shp1 abundance. Strain expressing endogenous ^{12xMyc}Met30, Shp1$^{3xHA-AID}$ and the F-Box protein ^{2xFLAG}OsTir under the constitutive ADH promoter were cultured at 30°C in YEPD medium in the absence and presence of 500µM auxin for the indicated time to gradually down-regulate endogenous Shp1-AID levels. Cells were exposed to 100 µM Cadmium and samples were harvested after 20 min. ^{12xMyc}Met30 was immunoprecipitated and co-precipitated Skp1 and Shp1-AID were analyzed by Western blot. Results shown in A, B and C are representative blots from three independent experiments. D) Densitometric analysis of Figure 4C shows a correlation between Shp1-AID abundance and Met30 dissociation from the core ligase during Cadmium stress. Purple line = Densitometric analysis of Western blot band intensities of Shp1-AID Totals. Time point 0 was set to 1. Turquoise line = Co-immunoprecipitated Skp1 signals were normalized to immunoprecipitated ^{12xMyc}Met30 signals to quantify F-box protein dissociation from the core ligase upon 20 min of cadmium exposure. Orange triangles correspond to the values obtained from Fig 1A and Suppl. Fig 1A quantifications of *shp1Δ.* Results shown in A, B and C are representative blots from three independent experiments**.**

Figure 1 - Shp1 is involved in the Cellular Response during Cadmium Stress

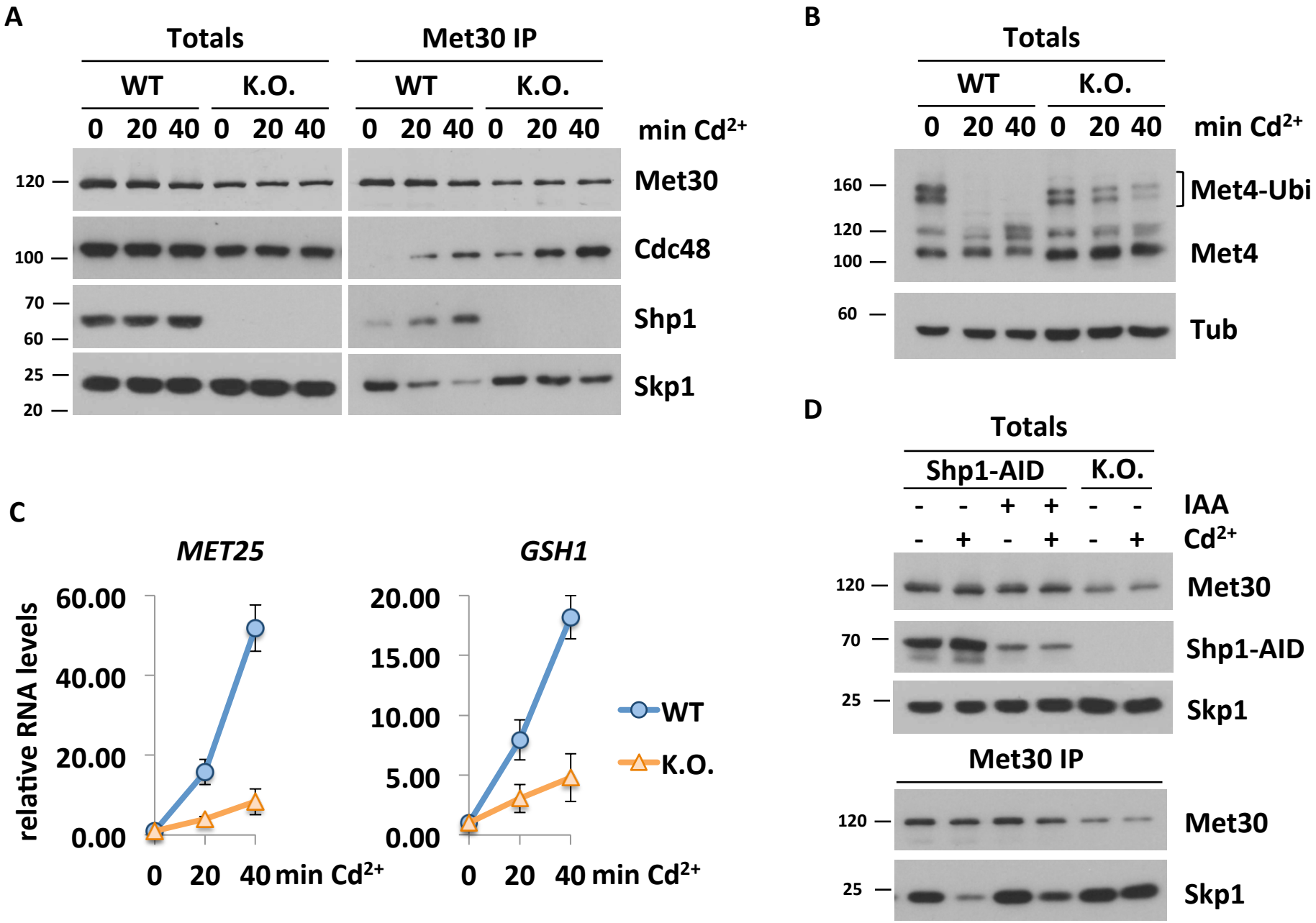

Figure 2 - Mutation of Functional Domains in Shp1

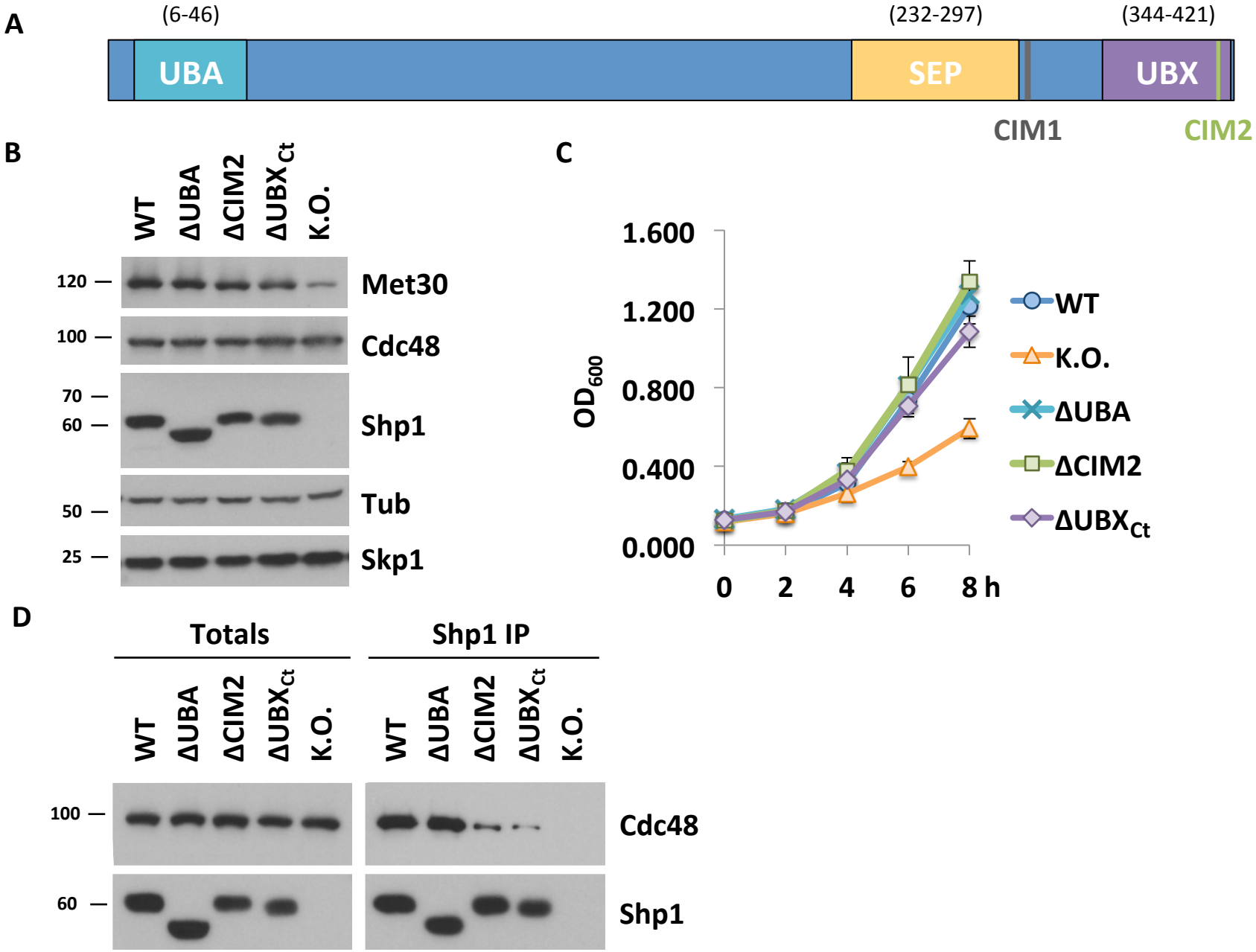

Figure 3 - UBX domain of Shp1 is required for SCF^{Met30} Disassembly during Cadmium Stress

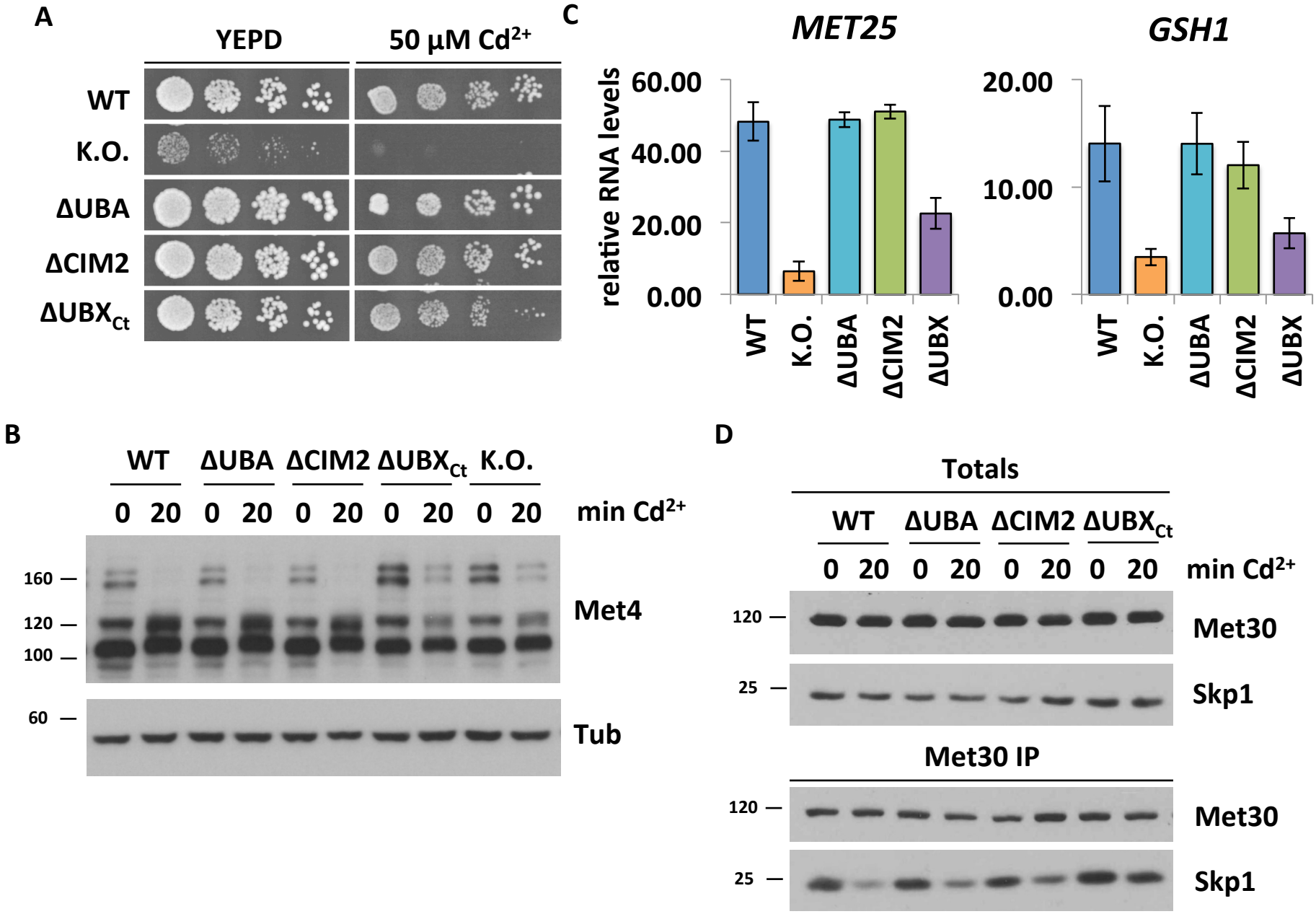

Figure 4 – Met30 Dissociation kinetics during Heavy Metal Stress are dependent on Shp1 Abundance

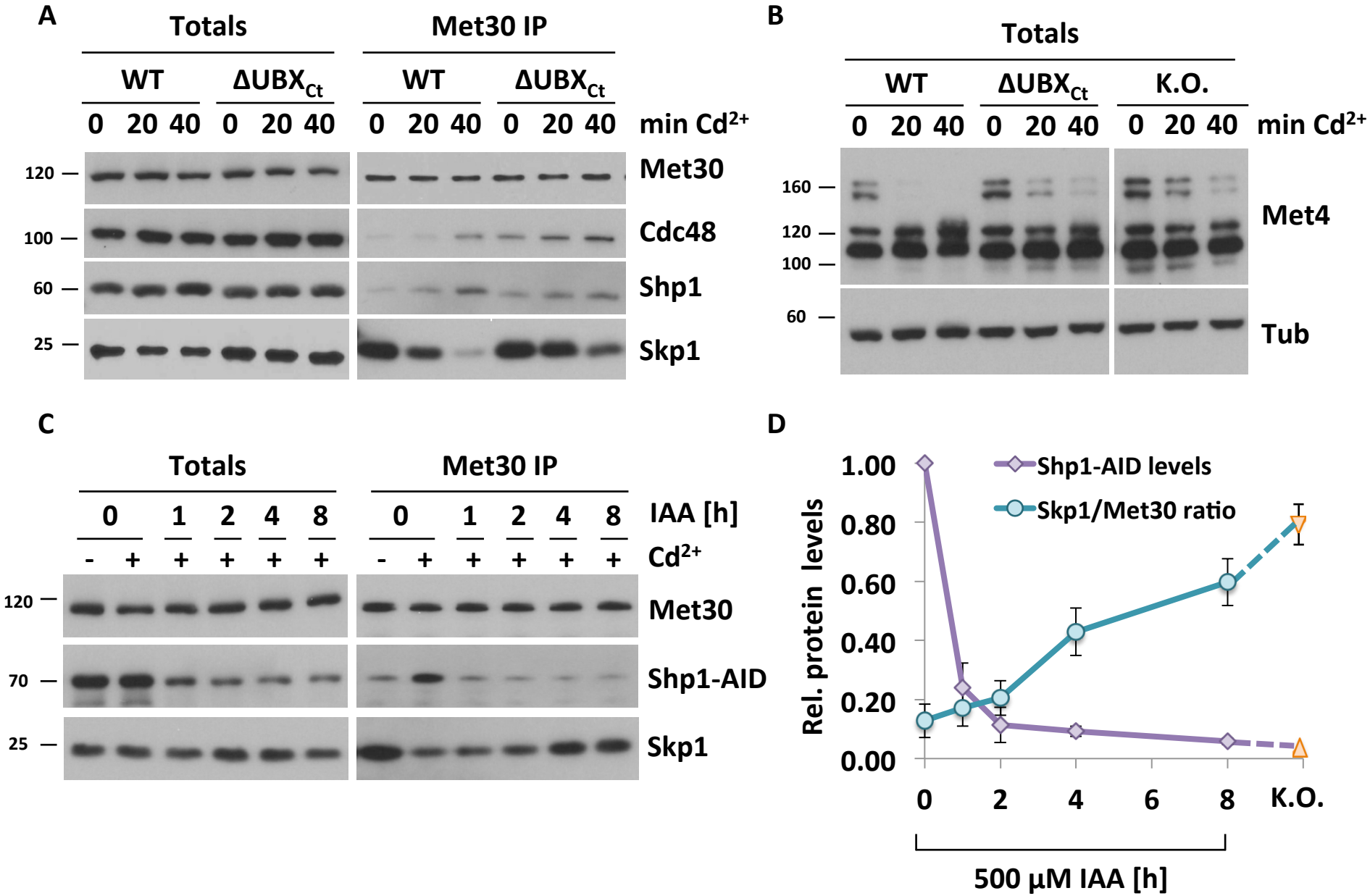

Suppl. Figure 1

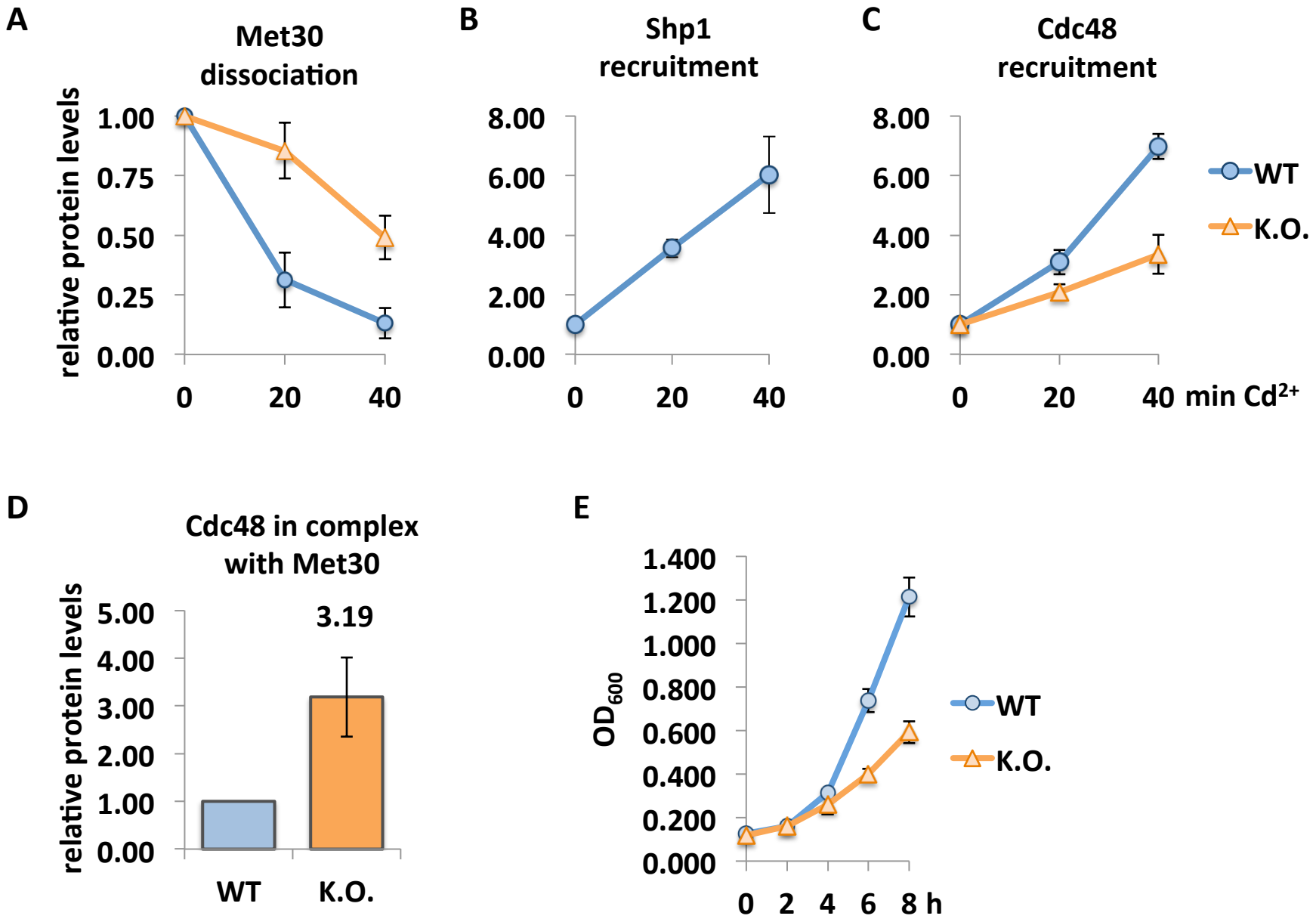

Suppl. Figure 1

F

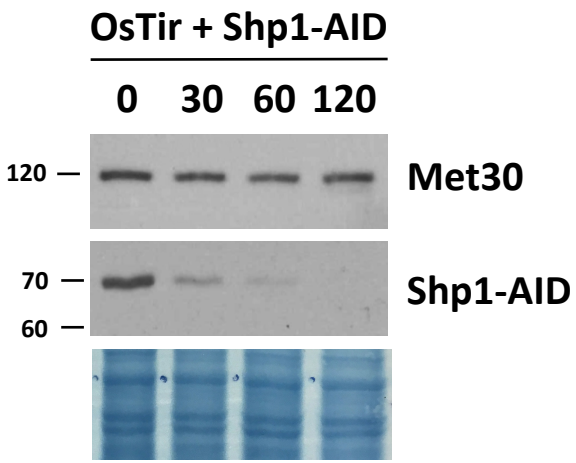

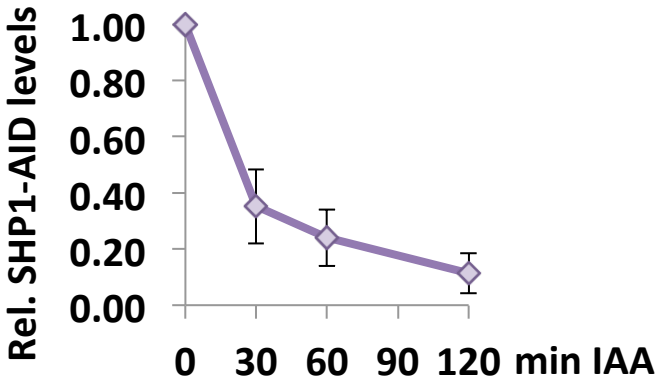

G

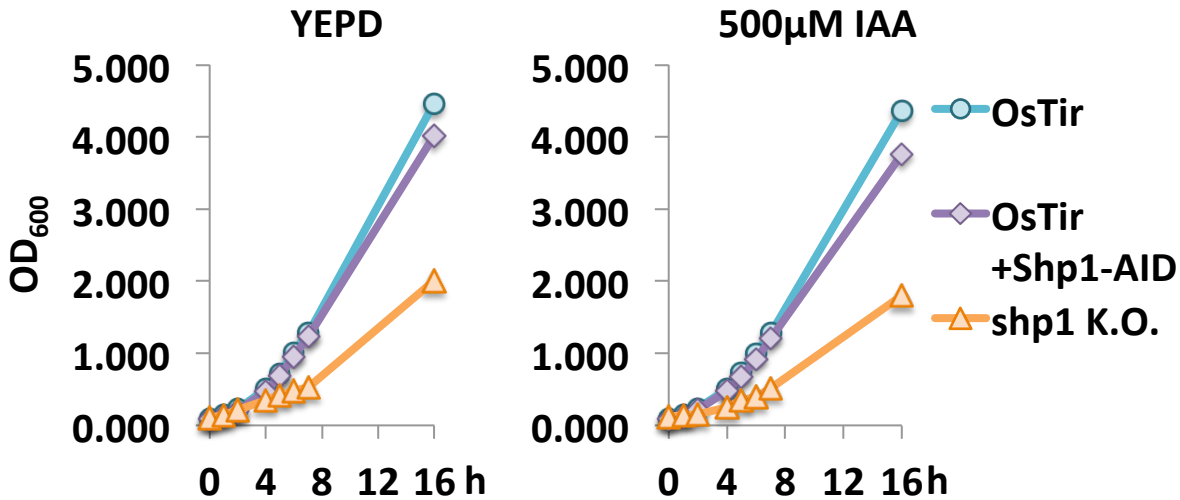

H

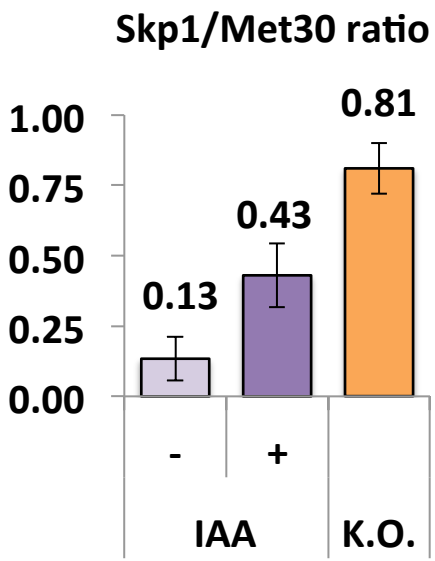

Suppl. Figure 2

A

MAEIP**DETIQQFMALTNVSHNIAVQYLSEFGDLNEALNSYYASQTD**DQKDRREEAHWNRQQEKAL **UBA**
KQEAFSTNSSNKAINTEHVGGLCPKPGSSQGSNEYLKRKGSTSPEPTKGSSRSGSGNNSRFMSFSDMV
RGQADDDDEDQPRNTFAGGETSGLEVTDPSDPNSLLKDLLEKARRGGQMGAENGFRDDEDHEMGA
NRFTGRGFRLGSTIDAADEVVEDNTSQSQRRPEKVTREI**TFWKEGFQVADGPLYRYDDPANSFYLSEL** **SEP**
NQGRAPLKLLDVQFGQEVEVNVYKKLDESYKAPTRK***LGGFSGQGQRL***GSPIPGESSPAEVPKNETPA **BS1/SHP motif → CIM1**
AQEQPMPDNEPK**QGDTSIQIRYANGKREVLHCNSTDTVKFLYEHVTSNANTDPSRNFTLNYAFPIKP** **UBX** **FPI → CIM2**
ISNDETTLKDADLLNSVVVQR*WA * (423 aa; 47kD) **Additional Cdc48 binding sites**

B

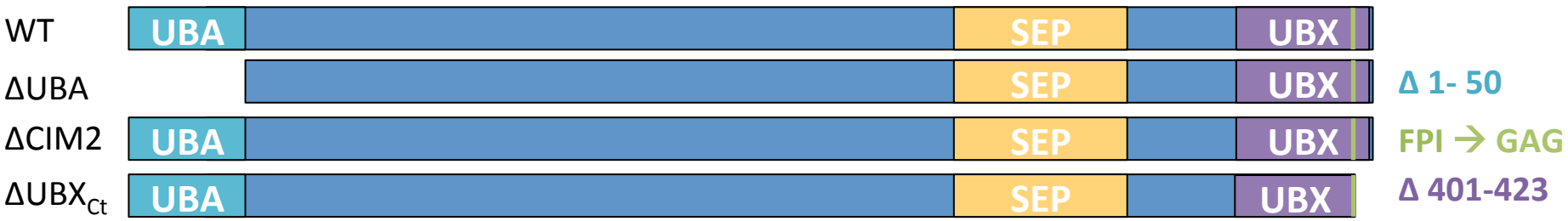

C

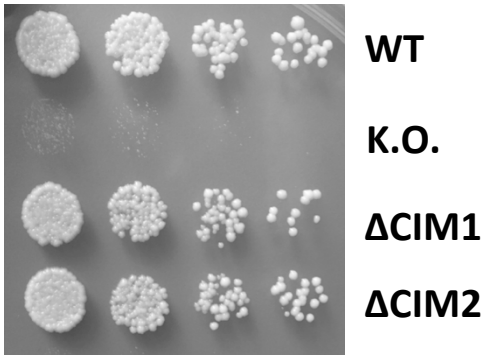

YEPD

D

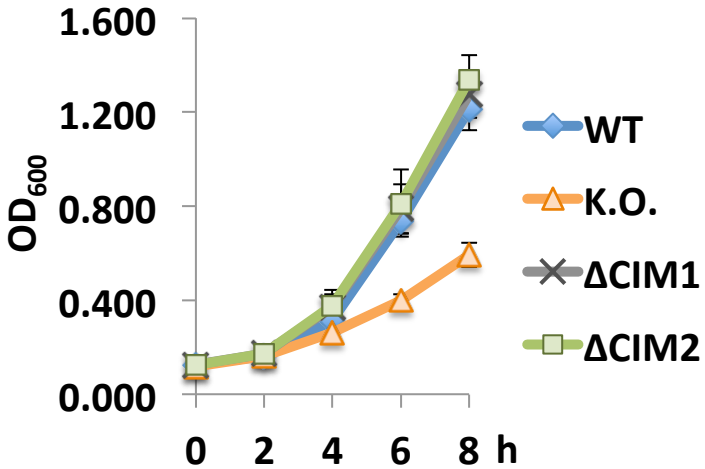

E

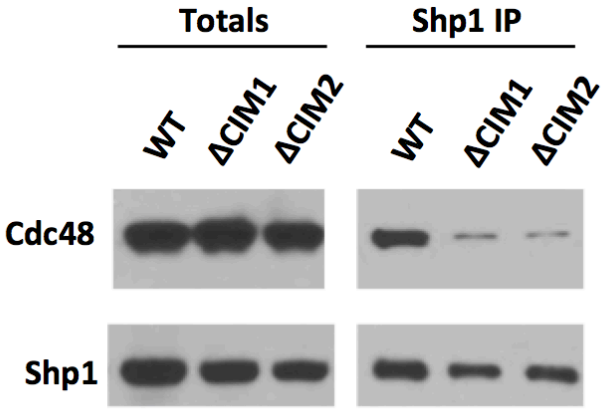

Suppl. Figure 2

F

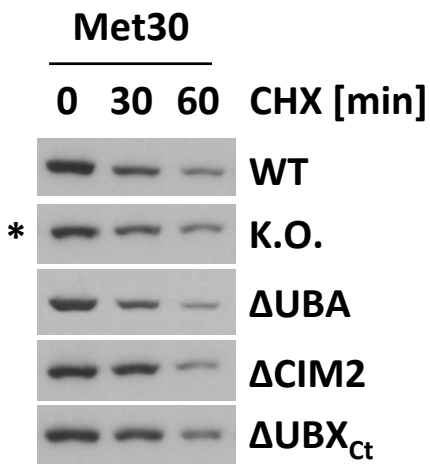

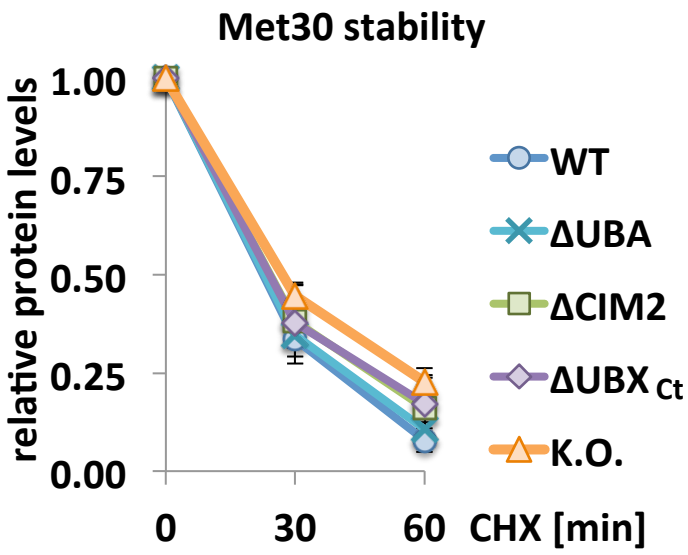

G

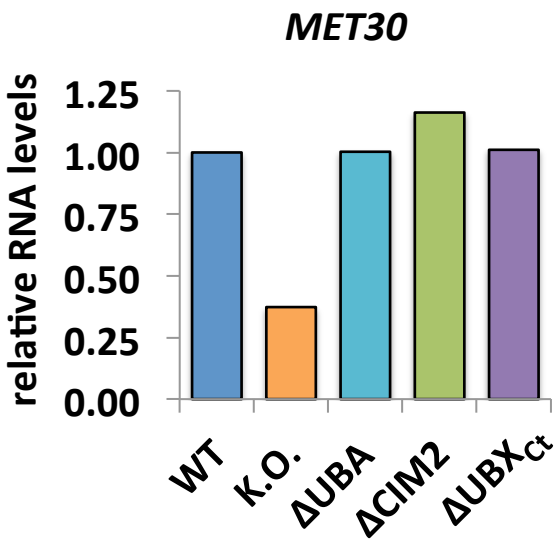

Suppl. Figure 3

A

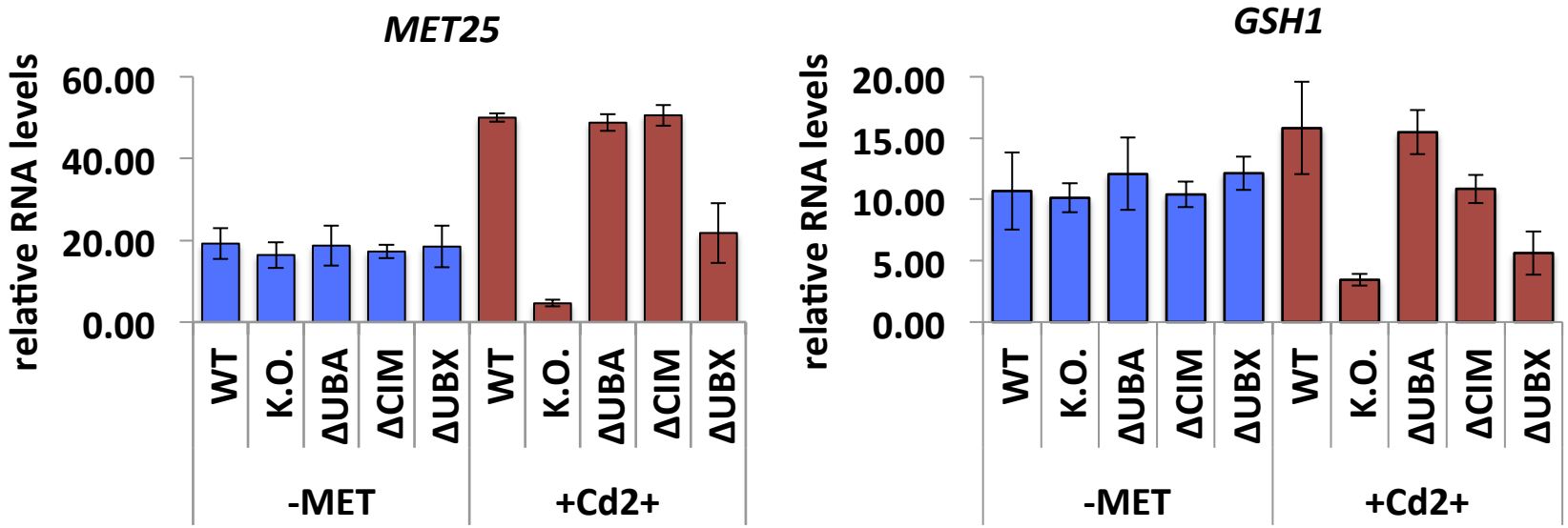

Suppl. Figure 4

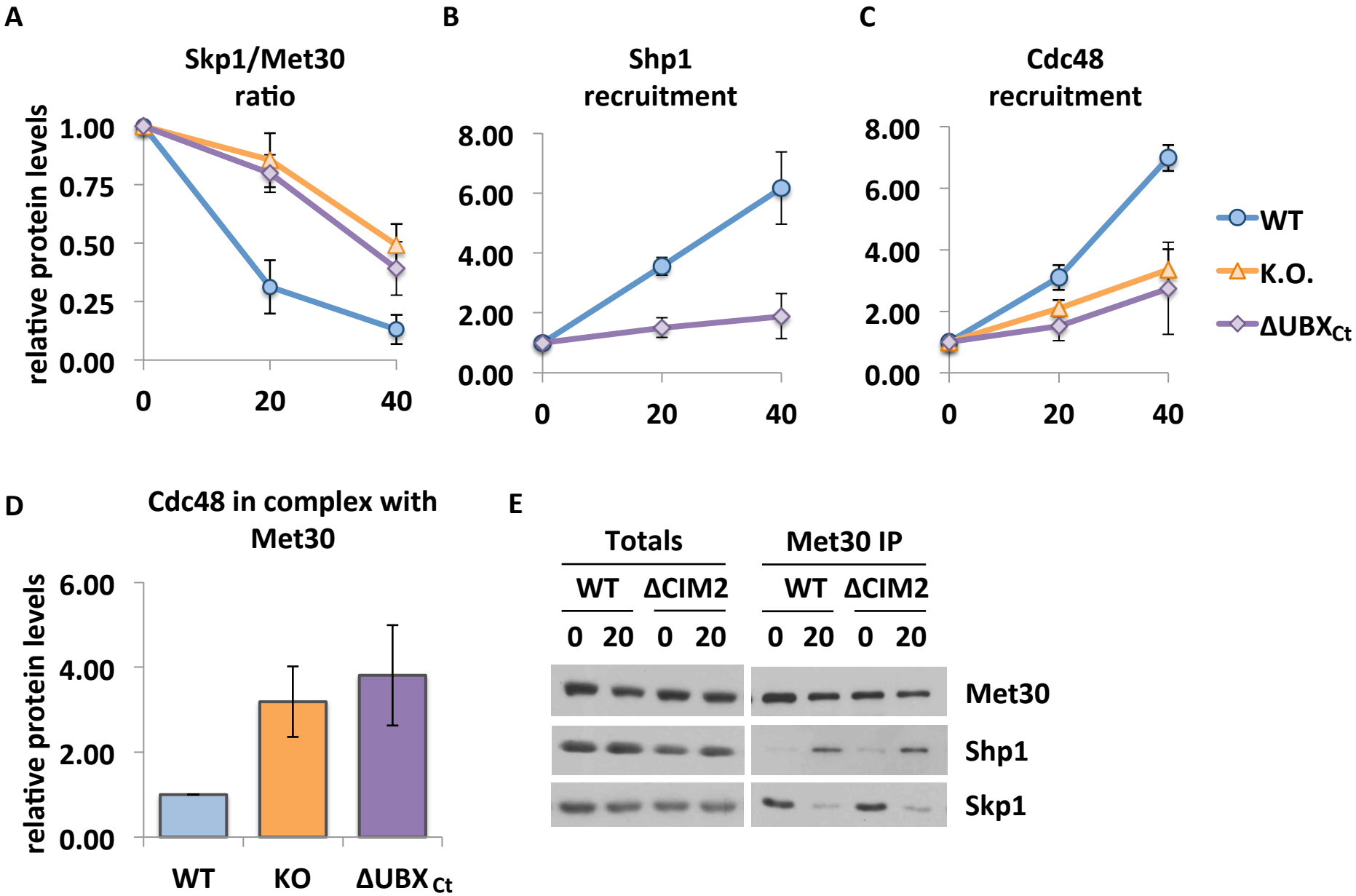

Suppl. Figure 4

F

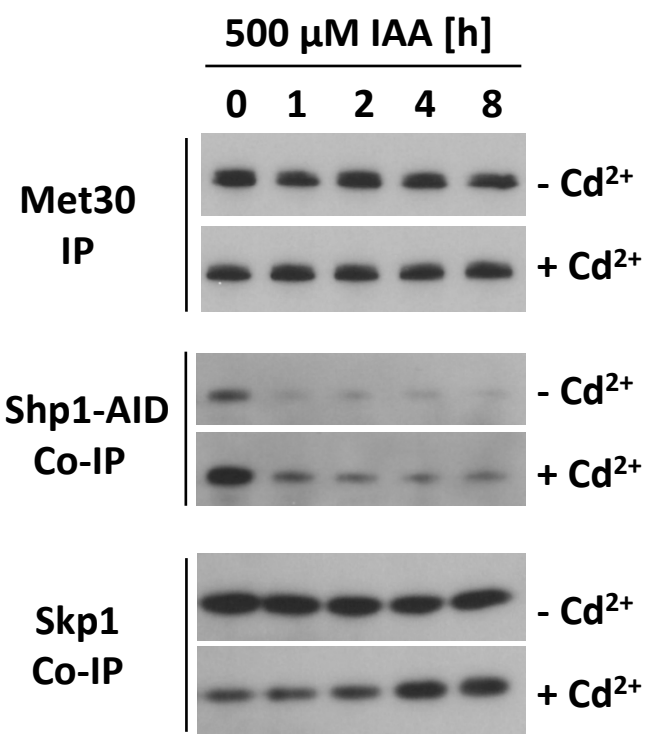

G

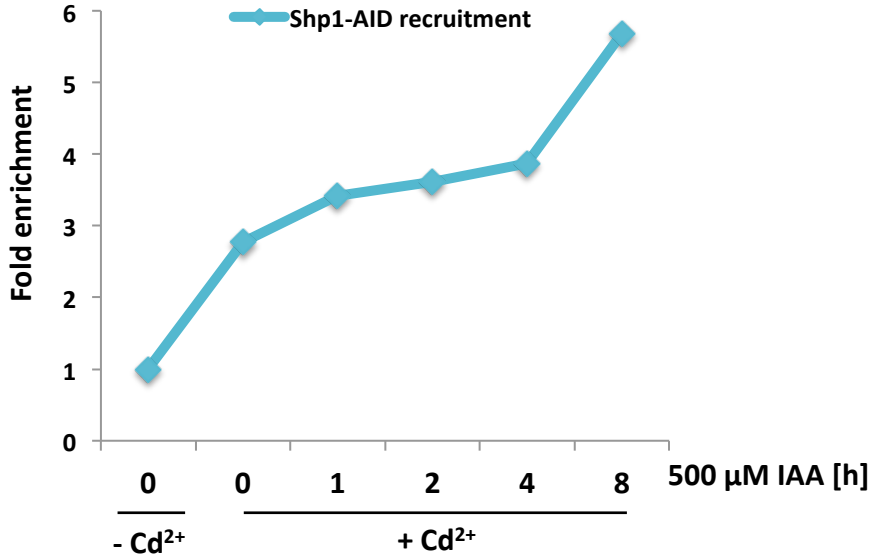

H

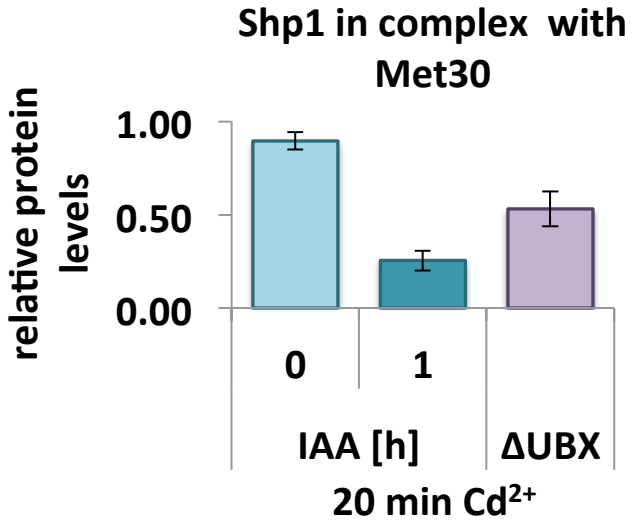

Suppl. Figure 5

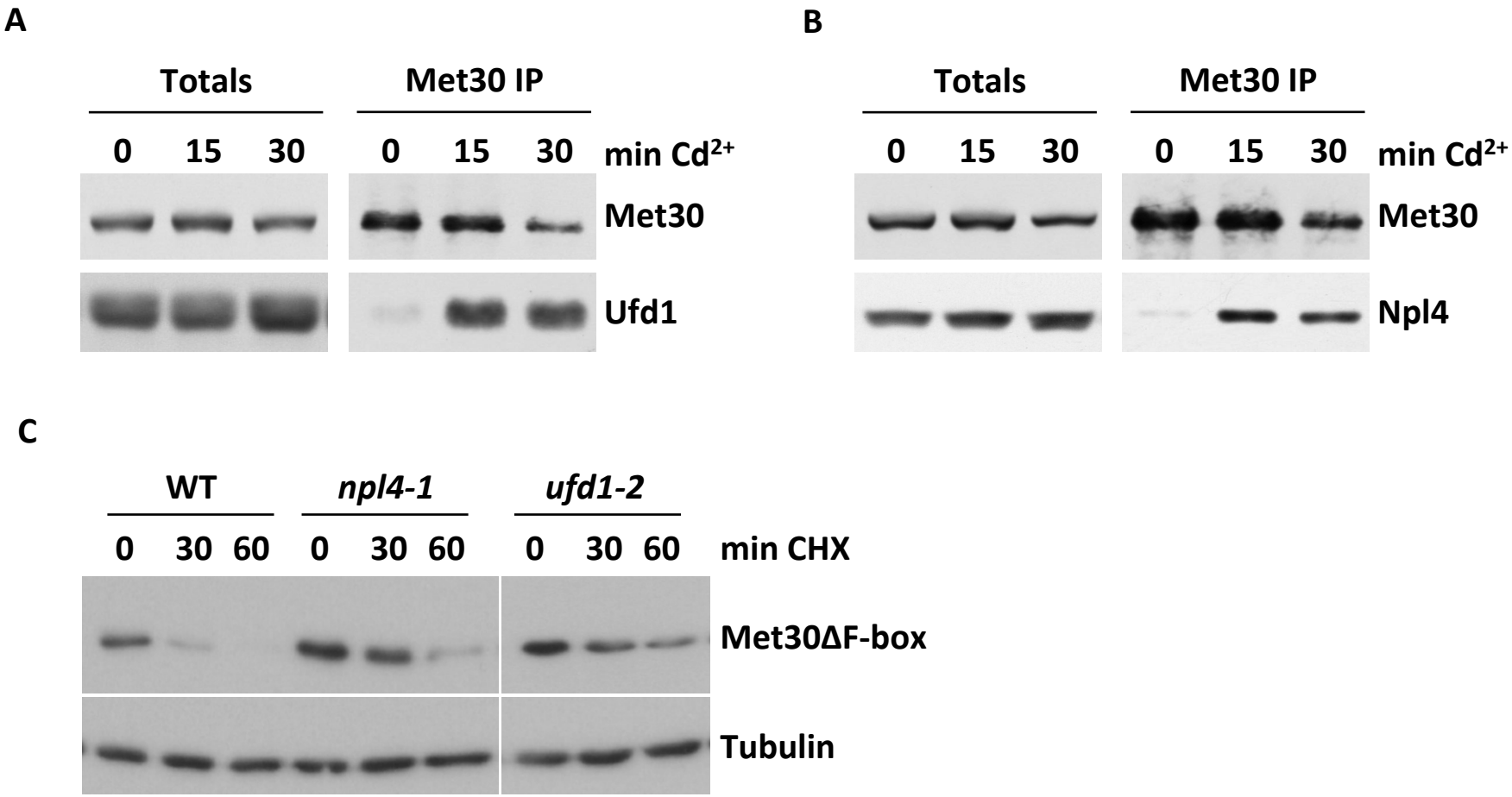

Supplemental Information

Supplemental Information includes five figures legends, Materials and Methods, Supplemental References and three Tables.

Supplementary Figure 1

Growth curves, dissociation and recruitment kinetics in WT, Shp1 knock out and Shp1-AID strains. A-C) Densitometric analysis of Western blot band intensities of immunoprecipitations in Fig 1A. For quantifications in A-C the signal intensities for each Shp1 variant at time point 0 were set to 1. A) Skp1 signals were normalized to ^{12xMyc}Met30 to quantify Met30 dissociation from the core ligase. B) Shp1^{3xHA} signals were normalized to ^{12xMyc}Met30 to determine recruitment of the UBX domain protein to SCF^{Met30}. Cdc48^{RGS6H} signals were normalized to ^{12xMyc}Met30 to resolve recruitment of the ATPase into SCF^{Met30}. D) Densitometry of Cdc48 ^{RGS6H} /^{12xMyc}Met30 ratio, WT at time point 0 was set to 1. E) *Shp1Δ* cells show a significant growth defect at 30°C. WT, and Shp1 K.O. strains were grown at 30°C in YEPD medium and samples were taken at indicated time points. Optic Density was measured at 600nm. F) Shp1-AID gets sufficiently down-regulated upon auxin exposure. Strains expressing endogenous ^{12xMyc}Met30, Shp1$^{3xHA-AID}$ and the F-Box protein ^{2xFLAG}OsTir under the constitutive ADH promoter were cultured at 30°C in YEPD. Samples were taken at indicated time-points after the addition of 500µM auxin (IAA). Protein levels were analyzed by Western blot, the amido black stain is shown as a loading control. G) Depicted strains do not show a significant growth defect at 30°C in the absence or presence of auxin. Strains were grown at 30°C in YEPD medium or YEPD containing 500 µM IAA and samples were taken at indicated time points. Optic Density was measured at 600nm. H) Densitometric analysis of Western blot band intensities of immunoprecipitations in Fig 1D. Skp1 signals were normalized to ^{12xMyc}Met30 to determine Met30 dissociation from the core ligase during cadmium stress.

Supplementary Figure 2

A) Amino Acid sequence of Shp1 - Specific domains/motifs are labeled and color-coded. B) Schematic of the most important Shp1 variants used throughout this study. C) Spotting assay - Serial dilutions of depicted strains were made and spotted onto YEPD plates. Plates were incubated for two days at 30°C. D) Shp1 WT, ΔCIM1 &2 and K.O. strains were grown at 30°C in YEPD medium and samples were taken at indicated time points. Optic Density was measured at 600nm. E) Cdc48 binding is significantly decreased but not abolished in ΔCIM1 and ΔCIM2. SHP1^{3xHA} variants were immunoprecipitated and co-precipitations of Cdc48^{RGS6H} were analyzed by Western blot. F) Met30 protein stability is unaffected in *shp1Δ* background. Depicted cultured were grown at 30°C in YEPD medium and Cycloheximide (100 µg/ml) was added and samples were collected at indicated time points. Protein stability was analyzed by immunoblotting followed by densitometric analysis. Asterisk next to Met30 levels of K.O. indicates longer exposure of the Western blot panel to show similar starting amounts of

Met30 in CHX time course. G) *MET30* RNA levels are decreased in *shp1Δ* cells. Depicted cultured were grown at 30°C in YEPD medium. RNA was extracted and expression of *MET30* was analyzed by RT-PCR and normalized to 18S rRNA levels.

Supplementary Figure 3

A) The expression of Met4-dependent genes in response to methionine starvation. Depicted yeast strains were grown at 30°C in YEDP medium to OD_{600} of 0.6. For Methionine starvation, cultures were washed with water and shifted to minimal medium without methionine for 30 minutes and then harvested. For heavy metal stress induction, cultures treated with 100 µM Cadmium and samples were harvested after 40 min exposure. RNA was extracted and expression of Met4 target genes *MET25* and *GSH1* was analyzed by RT-PCR and normalized to 18S rRNA levels (n=2).

Supplementary Figure 4

A-D) Quantification data of ΔUBX_{Ct} was integrated in the graphs shown in Suppl. Fig 1 A-D. For quantifications in A-C the signal intensity of each Shp1 variant at time point 0 was set to 1. A) co-immunoprecipitated Skp1 signals were normalized to immunoprecipitated ^{12xMyc}Met30 to quantify Met30 dissociation from the core ligase. B) Shp1^{3xHA} signals were normalized to ^{12xMyc}Met30. Then the ratio of co-immunoprecipitated Shp1^{+Cd}/Shp$^{w/o\ Cd}$ was determined to analyze recruitment of the UBX domain protein to SCF^{Met30}. Cdc48^{RGS6H} signals were normalized to ^{12xMyc}Met30. Next the ratio of co-immuniprecipitated Cdc48^{+Cd}/Cdc48$^{w/oCd}$ was analyzed to resolve recruitment of the ATPase into SCF^{Met30}. D) Densitometry of co-immunoprecipitated Cdc48 ^{RGS6H}/ immunoprecipitated ^{12xMyc}Met30 ratio, WT at time point 0 was set to 1. E) Shp1ΔCIM2 is recruited into SCF^{Met30} during cadmium stress. WT and *Shp1ΔCIM2* cells were cultured at 30°C in YEPD medium and treated with 100 µM Cadmium and samples were harvested after 20 min of exposure. ^{12xMyc}Met30 was immunoprecipitated and co-precipitated proteins were analyzed by Western blot. F) Full panel of immunoprecipitations that was partially shown in Fig 4C. Strain expressing endogenous ^{12xMyc}Met30, Shp1$^{3xHA-AID}$ and the F-Box protein ^{2xFLAG}OsTir under the constitutive ADH promoter was cultured at 30°C in YEPD medium in the absence and presence of auxin for the indicated time to gradually down-regulate endogenous Shp1-AID levels. Cells were exposed to 100 µM Cadmium and samples were harvested after 20 min. ^{12xMyc}Met30 was immunoprecipitated and co-precipitated Skp1 was analyzed by Western blot. G) Densitometric analysis of Western blot band intensities of immunoprecipitations in Suppl. Fig 4F. Shp1^{3xHA} signals were normalized to ^{12xMyc}Met30. Then the ratio of co-immunoprecipitated Shp1^{+Cd}/Shp$^{w/o\ Cd}$ was determined to follow Shp1 recruitment. H) Densitometry of Shp1^{3xHA}/^{12xMyc}Met30 ratio. Quantifications of Western blots shown in Fig. 4B and 4C.

Supplementary Figure 5

A&B) Cdc48 co-factors Ufd1 and Npl4 get recruited into SCFMet30 during heavy metal stress. Strains expressing endogenous ^{12xMyc}Met30, Skp1 and Ufd1^{3xHA} or Npl4^{3xHA} respectively were cultured at 30°C

in YEPD medium and treated with 100 µM Cadmium and samples were harvested at indicated time points. ^{12xMyc}Met30 was immunoprecipitated and co-precipitated proteins were analyzed by Western blot. C) Cdc48 cofactors Npl4 and Ufd1 are involved in 'Skp1-free' Met30 degradation. Wild type, npl4-1, and ufd1-2 temperature sensitive strains expressing ^{12myc}Met30ΔFbox were cultured at permissive temperature (25°C) and then shifted to non-permissive temperature (37°C) for 1.5 h. Cycloheximide (100 µg/ml) was added and samples were collected at the time intervals indicated. Met30ΔFbox protein stability was analyzed by immunoblotting with anti-myc antibodies. Tubulin was used as a loading control.

Methods

Plasmids, Yeast Strains and Growth Conditions

Yeast strains used in this study are isogenic to 15DaubD, a bar1D ura3Dns, a derivative of BF264-15D (1). Specific strains are listed in Table S1. The 9xMYC tag of pADH_OsTir9xMYC::URA (2) was exchanged with a 2xFLAG tag by amplification of the vector using primers 1&2 (table S3). The PCR fragment was digested with BamHI and ligated to generate pADH_OsTir2xFLAG::URA. The plasmid was linearized with StuI and transformed into yeast strain PY1. Next, The AID-fragment was amplified from the pKAN-pCUP1-9xMYC-AID plasmid using primers 3&4 (table S3) and inserted via Gibson Assembly into the AscI linearized pFA6a-3xHA::TRP plasmid to generate the tagging vector pFA6a-3xHA-AID::TRP. A PCR fragment using primers 13&14 (table S3) was amplified and transformed into PY1+pADH_OsTir2xFLAG::URA. This strain was transformed with YCpLEUpmet30_9xMYCMET30 to generate PY2230. For CRISPR/Cas9 edited yeast strains the vector pML107 (3) which contain both sgRNA and Cas9 expression cassettes was used. To generate the guide RNA sequences the "CRISPR Toolset" (http://wyrickbioinfo2.smb.wsu.edu/crispr.html) was consulted. pML107 was linearized using SwaI and hybridized primers for guideRNAs as shown in table S3 were inserted via Gibson Assembly to generate pML107-Shp1 vectors (table S2). The vectors were transformed together with the hybridized 90mer oligos containing the Shp1-specific repair sequence into PY1630 to generate marker-free Shp1::3xHA mutants shown in table S1. All other strains used were generated using classic PCR based gene modification methods (4). Generated plasmids and strains were verified by sequencing. All strains were cultured in standard media, and standard yeast genetic techniques were used unless stated otherwise (5). References to the use of cadmium (Cd^{2+}) are specifically to cadmiumchloride ($CdCl_2$). For cell spotting assays, strains were cultured to logarithmic growth phase, sonicated and then counted. Serial dilutions were made and spotted onto YEPD plates supplemented with or without indicated amounts of cadmium via a pin replicator (V&P Scientific, San Diego, CA).

Protein Analysis

For Western blot analysis and immunoprecipitation assays, yeast whole cell lysates were prepared under native conditions in Triton X-100 buffer 50mM HEPES, pH 7.5, 0.2% Triton X-100, 200mM NaCl, 10% glycerol, 1mM dithiothreitol, 10mM Na-pyrophosphate, 5mM EDTA, 5mM EGTA, 50mM NaF,

0.1mM orthovanadate, 1mM phenylmethylsulfonyl floride [PMSF], and 1µg/ml each leupeptin, and pepstatin). Cells were homogenized in a screw-cap tube with 0.5 mm glass beads and Antifoam Y-30 using a MP FastPrep 24 (speed 4.0, 3x20 sec). Lysates were separated from glass beads and transferred into 1.5 ml reaction Tube (USA Scientific). Lysates were cleared by centrifugation (10 min, 14000g at 4°). For Western blot analysis proteins were separated by SDS-PAGE and transferred to a polyvinylidene difluoride (PVDF) membrane. Proteins were detected with the following primary antibodies: anti-Met4 (1:20000; a gift from M. Tyers), anti-Skp1 (1:5000; a gift from R. Deshaies), anti-Cdc48 (1:20000; a gift from E. Jarosch), anti-Myc (1:2000; Santa Cruz, 9E10), anti-HA (1:2000; Santa Cruz, F7) anti-RGS6H (1:2000; QIAGEN, Germantown, MD) anti-Tubulin (1:2000; Santa Cruz). Western blots results shown are representative blots from three experiments with independent cultures. Band intensities of immunoblots were quantified using either ImageJ or the Biorad Image Lab software. For immunoprecipitation of 9xMYC tagged proteins, 1 mg of total protein lysate was incubated with in Triton X-100 buffer equilibrated MYC-trap beads (Chromotek) in a final volume of 500 µl over night at 4°C on a nutator. The next day beads and supernatants were separated by centrifugation (2 min, 100g at 4°C). Beads were washed 3 times in 1 ml Triton X-100 buffer plus inhibitors at 4°C. Beads were resuspended in 2x Laemmli buffer and boiled for 5 min at 95°C to elute proteins. For immunoprecipitation of 3xHA tagged proteins, 1 mg of total protein lysate in a final volume of 500 µl was incubated with 1 µg of anti-HA Y-11 (Santa Cruz, discontinued) for 2 hours at 4°C on a nutator. In Triton X-100 buffer equilibrated Protein A Sepharose (Sigma-Aldrich) was added and incubated over night at 4°C on a nutator. The next day beads and supernatants were separated by centrifugation (2 min, 100g at 4°C). Beads were washed 3 times in 1 ml Triton X-100 buffer plus inhibitors at 4°C. Beads were resuspended in 2x Laemmli buffer and boiled for 5 min at 95°C to elute proteins.

RNA and RT-PCR

Yeast RNA was prepared using the RNeasy Plus Mini Kit (Quiagen) according to the manufacturers protocol. cDNA synthesis was performed using Super Sript II Reverse Transcriptase Kit (Invitrogen). 1.5 µg of RNA was transcribed into cDNA according to the manufacturers protocol. The synthesized cDNA was diluted 1:15 in Nuclease-free water. RT-PCR was performed on a Biorad CFX Connect RT-PCR machine using the Biorad iTaq Universal SYBR Green SuperMix and 4 µl of the cDNA 1:15 dilution were use for a 20µl reaction as a template. Primers were used in a final concentration of 0.2 µM. Sequences of primers are: *MET25F* GCCACCACTTCTTATGTTTTCG, *MET25R* AGCAGCAGCACCACCTTC, *GSH1F* TGACAGCATCCATCAGGACCAG, *GSH1R* GGAAGCCAGTTTCGCCTCTTTG, 18SrRNAF GTGGTGCTAGCATTTGCTGGTTAT, 18SrRNAR CGCTTACTAGGAATTCCTCGTTGAA. 18S rRNA was used as a normalization control for each sample. The ΔΔCt method was used for analysis. Data are represented as mean ±SD.

Supplemental References

1. S. I. Reed, J. A. Hadwiger, A. T. Lorincz, Protein kinase activity associated with the product of the yeast cell division cycle gene CDC28. *Proc. Natl. Acad. Sci. U. S. A.* (1985) https:/doi.org/10.1073/pnas.82.12.4055.
2. M. Morawska, H. D. Ulrich, An expanded tool kit for the auxin-inducible degr on system in budding yeast. **4**, 1–4.
3. M. F. Laughery, *et al.*, New vectors for simple and streamlined CRISPR-Cas9 genome editing in Saccharomyces cerevisiae. *Yeast* (2015) https:/doi.org/10.1002/yea.3098.
4. M. S. Longtine, *et al.*, Additional modules for versatile and economical PCR-based gene deletion and modification in Saccharomyces cerevisiae. *Yeast* (1998) https:/doi.org/10.1002/(SICI)1097-0061(199807)14:10<953::AID-YEA293>3.0.CO;2-U.
5. , Guide to yeast genetics and molecular biology. in *Methods in Enzymology*, (1991) https:/doi.org/10.2307/3760517.

Table S1

Strain	**relevant genotype**	**Source**
15Daub	a bar1Δ ura3Δns, ade1 his2 leu2-3112 trp1-1	Reed et al., 1985
PY236	*pep4::URA3*	Kaiser et al., 2000
PY1073	*12mycMET30::ZEO pep4::URA3*	Yen et al.; 2012
PY1630	*CDC48RGS6xHis::KAN 12MycMET30::ZEO pep4::URA*	Yen et al.; 2012
PY1729	*CDC48RGS6xHis::KAN 12MycMET30::ZEO Shp1::HYG pep4::URA*	Yen et al.; 2012
PY2230	*2xFLAGOsTir::URA Shp13xHA_AID::TRP YCpLEUprmet30_9xMYCMET30*	This Study
PY2231	*CDC48RGS6xHis::KAN 12MycMET30::ZEO Shp13xHA::TRP pep4::URA*	This Study
PY2232	*CDC48RGS6xHis::KAN 12MycMET30::ZEO Shp13xHA ΔUBA pep4::URA*	This Study
PY2234	*CDC48RGS6xHis::KAN 12MycMET30::ZEO Shp13xHA ΔCIM1::TRP pep4::URA*	This Study
PY2235	*CDC48RGS6xHis::KAN 12MycMET30::ZEO Shp13xHA ΔCIM2::TRP pep4::URA*	This Study
PY2236	*CDC48RGS6xHis::KAN 12MycMET30::ZEO Shp13xHA ΔUBX::TRP pep4::URA*	This Study

Table S2

Plasmid	relevant genotype	Source
pP491	*pFa6a3xHA::TRP*	Longtine et al., 1998
pP699	*YCpLEUpmet30_9xMYCMET30*	Flick et al., 2006
p1716	*pADH_OsTir9xMYC::URA*	Ulrich et al,; 2013
pP1216	*pADH_OsTir2xFLAG::URA*	This Study
p1736	pKAN-pCUP1-9xMYC-AID	Ulrich et al,; 2013
pP1217	pFa6a3xHA_AID::TRP	This Study
pML107	pSNR52sgRNA casette CAS9-gWY001 casette LEU2	Laughery et al.; 2015
pML107gShp1ΔUBA	pSNR52sgRNA shp1 -13 casette CAS9-gWY001 casette LEU2	This Study
pML107gShp1ΔCIM1	pSNR52sgRNA shp1 907 casette CAS9-gWY001 casette LEU2	This Study
pML107gShp1ΔCIM2	pSNR52sgRNA shp1 1184 casette CAS9-gWY001 casette LEU2	This Study

Table S3

No	Primer	Sequence	used for
1	OsTir-2xFLAG BamHI F	AAAggatccGACTACAAAGACGATGATGACAAAGACTACAAAGACGATGATGACAAATAAagatctcggccgccacc	pMK_2xFLAGOsTir
2	OsTir-2xFLAG BamHI R	TTTggatccagcaccTAGGATTTTAACAAAATTTGGTGCATCATCCC	
3	AID in pFa6a3xHA::TRP F	TACGCTGCTCAGTGCCCTAAAGATCCAGCCAAACCTCC	pFa6a3xHA_AID::TRP
4	AID in pFa6a3xHA::TRP R	TAGAAGTGGCGCGCCTCAACCAGCTCCCAAGTCCTTAGATT	
5	shp1 -13 gRNA F	GAAAGATAAATGATCAATTAACTCATTATTTAGGTAGTTTTAGAGCTAGAAATAGCAAGTTAAAA	pML107gShp1ΔUBA
6	shp1 -13 gRNA F	TTTTAACTTGCTATTTCTAGCTCTAAAACTACCTAAATAATGAGTTAATTGATCATTTATCTTTC	
9	shp1 907 gRNA F	GAAAGATAAATGATCACTGGGCGGTTTTTCAGGCCAGTTTTAGAGCTAGAAATAGCAAGTTAAAA	pML107gShp1ΔCIM1
10	shp1 907 gRNA R	TTTTAACTTGCTATTTCTAGCTCTAAAACTGGCCTGAAAAACCGCCCAGTGATCATTTATCTTTC	
11	shp1 1184 gRNA F	GAAAGATAAATGATCAGCTTATTGGTTTGATAGGAAGTTTTAGAGCTAGAAATAGCAAGTTAAAA	pML107gShp1ΔCIM2
12	shp1 1184 gRNA R	TTTTAACTTGCTATTTCTAGCTCTAAAACTTCCTATCAAACCAATAAGCTGATCATTTATCTTTC	
13	PK1126 SHP1 Cterm tagging 5´	CGCTGATCTG CTGAACTCCG TTGTCGTGCA AAGATGGGCA CGGATCCCCG GGTTAATTAA	SHP1-3xHA
14	PK1127 SHP1 Cterm tagging 3´	GTTGAAGTCT TTTCCCGTTT CTGTTTTTGT ATATTTATGC GAATTCGAGC TCGTTTAAAC	
15	PK1098 SHP1 KO 5'	AGAAACGTCG GTAGCACAAC AATTAACTCA TTATTTAGGT CGGATCCCCG GGTTAATTAA	K.O.
16	PK1099 SHP1 KO 3'	GTTGAAGTCT TTTCCCGTTT CTGTTTTTGT ATATTTATGC GAATTCGAGC TCGTTTAAAC	
17	Shp1ΔUBA F	TATATAAGAAACGTCGGTAGCACAACAATTAACTCATTATTTATGAGAGAGGAAGCACATTGGAACAGACAGCAGGAGAAGGCCCTCAAG	UBA
18	Shp1ΔUBA R	CTTGAGGGCCTTCTCCTGCTGTCTGTTCCAATGTGCTTCCTCTCTCATAAATAATGAGTTAATTGTTGTGCTACCGACGTTTCTTATATA	
21	Shp1ΔCIM1 F	tataaaaaattagatgagtcttataaagctccgacgagaaaaGCGG	CIM1

		CCGCTggatctcctatcccgggtgaatcgtcacctgcggaggttcca	
22	Shp1ΔCIM1 R	tggaacctccgcaggtgacgattcacccgggataggagatccAGCG GCCGCttttctcgtcggagctttataagactcatctaatttttata	
23	Shp1ΔCIM2 F	gaacactgacccatcgaggaatttcaccttgaattatgcTGGtGctG GTaaaccaataagcaacgatgagacaacattgaaggacgctg	
24	Shp1ΔCIM2 R	cagcgtccttcaatgttgtctcatcgttgcttattggtttACCagCaCC Agcataattcaaggtgaaattcctcgatgggtcagtgttc	CIM2
25	ShpΔUBX F	tgacccatcgaggaatttcaccttgaattatgcTtttcctatcaaaCC AATAtAGCAACGATGAGACAACattgaaggacgctga	
26	ShpΔUBX R	tcagcgtccttcaatGTTGTCTCATCGTTGCTaTATTGGtttg ataggaaaAgcataattcaaggtgaaattcctcgatgggtca	UBX